

Sakaue et al.

## 1 A statistical genetics guide to identifying HLA alleles driving complex 2 disease

3  
4 Saori Sakaue<sup>1,2,3</sup>, Saisriram Gurajala<sup>1,2,3</sup>, Michelle Curtis<sup>1,2,3</sup>, Yang Luo<sup>1,2,3</sup>, Wanson Choi<sup>4</sup>,  
5 Kazuyoshi Ishigaki<sup>1,2,3,5</sup>, Joyce B. Kang<sup>1,2,3,6</sup>, Laurie Rumker<sup>1,2,3,6</sup>, Aaron J. Deutsch<sup>3,7,9</sup>,  
6 Sebastian Schönherr<sup>10</sup>, Lukas Forer<sup>10</sup>, Jonathon LeFaive<sup>11,12</sup>, Christian Fuchsberger<sup>10-13</sup>, Buhm  
7 Han<sup>4,14</sup>, Tobias L. Lenz<sup>15</sup>, Paul I. W. de Bakker<sup>16</sup>, Albert V. Smith<sup>11,12</sup>, Soumya  
8 Raychaudhuri<sup>1,2,3,6,17</sup>

- 9  
10 1. Center for Data Sciences, Brigham and Women's Hospital, Harvard Medical School, Boston, MA,  
11 USA  
12 2. Divisions of Genetics and Rheumatology, Department of Medicine, Brigham and Women's  
13 Hospital, Harvard Medical School, Boston, MA, USA  
14 3. Program in Medical and Population Genetics, Broad Institute of MIT and Harvard, Cambridge,  
15 MA, USA  
16 4. Department of Biomedical Sciences, Seoul National University College of Medicine, Seoul,  
17 South Korea  
18 5. Laboratory for Human Immunogenetics, RIKEN Center for Integrative Medical Sciences,  
19 Yokohama, Japan  
20 6. Department of Biomedical Informatics, Harvard Medical School, Boston, MA, USA  
21 7. Diabetes Unit, Massachusetts General Hospital, Harvard Medical School, Boston, MA, USA  
22 8. Center for Genomic Medicine, Massachusetts General Hospital, Harvard Medical School,  
23 Boston, MA, USA  
24 9. Program in Metabolism, Broad Institute of MIT and Harvard, Cambridge, MA, USA  
25 10. Institute of Genetic Epidemiology, Department of Genetics, Medical University of Innsbruck,  
26 Innsbruck, Austria  
27 11. Center for Statistical Genetics, University of Michigan School of Public Health, Ann Arbor, MI,  
28 USA  
29 12. Department of Biostatistics, University of Michigan School of Public Health, Ann Arbor, MI, USA  
30 13. Institute for Biomedicine, Eurac Research, Bolzano, Italy  
31 14. Interdisciplinary Program in Bioengineering, Seoul National University, Seoul, South Korea  
32 15. Research Unit for Evolutionary Immunogenomics, Department of Biology, University of Hamburg,  
33 Hamburg, Germany  
34 16. Vertex Pharmaceuticals, Boston, MA, USA  
35 17. Centre for Genetics and Genomics Versus Arthritis, University of Manchester, Manchester, UK  
36

37 \*Address correspondence to:

38 Soumya Raychaudhuri  
39 77 Avenue Louis Pasteur, Harvard New Research Building, Suite 250D  
40 Boston, MA 02446, USA.  
41 [soumya@broadinstitute.org](mailto:soumya@broadinstitute.org)  
42 617-525-4484 (tel); 617-525-4488 (fax)

Sakaue et al.

43 **Abstract**

44 The human leukocyte antigen (HLA) locus is associated with more human complex diseases  
45 than any other locus. In many diseases it explains more heritability than all other known loci  
46 combined. Investigators have now demonstrated the accuracy of *in silico* HLA imputation  
47 methods. These approaches enable rapid and accurate estimation of HLA alleles in the millions  
48 of individuals that are already genotyped on microarrays. HLA imputation has been used to  
49 define causal variation in autoimmune diseases, such as type I diabetes, and infectious  
50 diseases, such as HIV infection control. However, there are few guidelines on performing HLA  
51 imputation, association testing, and fine-mapping. Here, we present comprehensive statistical  
52 genetics guide to impute HLA alleles from genotype data. We provide detailed protocols,  
53 including standard quality control measures for input genotyping data and describe options to  
54 impute HLA alleles and amino acids including a web-based Michigan Imputation Server. We  
55 updated the HLA imputation reference panel representing global populations (African, East  
56 Asian, European and Latino) available at the Michigan Imputation Server ( $n = 20,349$ ) and  
57 achieved high imputation accuracy (mean dosage correlation  $r = 0.981$ ). We finally offer best  
58 practice recommendations to conduct association tests in order to define the alleles, amino  
59 acids, and haplotypes affecting human traits. This protocol will be broadly applicable to the  
60 large-scale genotyping data and contribute to defining the role of *HLA* in human diseases  
61 across global populations.

Sakaue et al.

62 **Main**

63 **Introduction**

64 More than 50 years ago, some of the earliest complex human disease genetic associations  
65 were reported within the major histocompatibility complex (MHC) locus<sup>1,2</sup>. This locus has since  
66 been mapped to the short arm of chromosome 6. Sequencing of the human genome has  
67 revealed that the MHC locus consists of a cluster of more than 200 genes, including many with  
68 immune functions<sup>3</sup>. The MHC locus is broadly divided into three subclasses: the class I region  
69 (e.g., *HLA-A*, *HLA-B* and *HLA-C* genes), the class II region (e.g., *HLA-DPA1*, *HLA-DPB1*,  
70 *HLA-DQA1*, *HLA-DQA2*, *HLA-DQB1*, *HLA-DQB2*, *HLA-DRA*, *HLA-DRB1*, *HLA-DRB2*,  
71 *HLA-DRB3*, *HLA-DRB4* and *HLA-DRB5* genes), and the class III region, which contains  
72 additional genes implicated in immune and inflammatory responses (e.g., complement genes)<sup>4</sup>  
73 (**Figure 1a**). Those *HLA* class I and II genes encode protein molecules that form complexes  
74 that present antigenic peptides to T cells, thereby influencing thymic selection and T cell  
75 activation<sup>4</sup> (**Figure 1b**). The functional importance of the *HLA* genes and the highly polymorphic  
76 nature of this locus have made the MHC region confer the largest number of disease  
77 associations of any locus genome-wide (**Figure 1c**). MHC-disease risk is modulated by several  
78 underlying mechanisms. For example, in rheumatoid arthritis, polymorphisms in the amino acid  
79 sequence of *HLA-DRB1* change the capability of presenting autoantigens<sup>5</sup> or increase the  
80 autoreactive T cells during thymic selection<sup>6</sup>. In another example, the *HLA-C\*06:02* allele is  
81 associated with psoriasis, probably due to increased CD8+ T-cell mediated inflammatory  
82 reactions<sup>7</sup>. In another example, schizophrenia's association within MHC locus was explained in

Sakaue et al.

83 part by structural variation in *C4*, which might modulate synaptic elimination during  
84 development<sup>8</sup>.

85 The *HLA* genes within the MHC have been difficult to study because of their highly  
86 polymorphic nature, the region's complex relationship with natural selection, and its unique  
87 long-range linkage disequilibrium (LD) structure. The highly polymorphic nature of *HLA* genes  
88 renders traditional probe-based genotyping to be challenging. In addition, the genetic diversity  
89 at *HLA* genes is highly population-specific, necessitating efforts to accurately genotype *HLA*  
90 alleles and investigate phenotypic associations in global populations.

91 These challenges have driven high interest in the genetics community to develop and  
92 deploy statistical techniques for *HLA* alleles. While the direct typing of *HLA* alleles continues to  
93 be costly, labor-intensive and unscalable, *in silico* *HLA* imputation has recently enabled rapid  
94 and accurate estimation of *HLA* alleles in individuals already genotyped on microarrays.  
95 However, there are few guidelines for *HLA* imputation and to estimate and fine-mapping; these  
96 methods are necessary to define *HLA* effects on human diseases, especially in biobank-scale  
97 data from multiple populations.

98 In this context, here we provide detailed guidelines for imputing *HLA* alleles and testing for  
99 an association with human diseases and traits, in large-scale cohorts and global biobanks. We  
100 also provide a step-by-step online tutorial with scripts and available software  
101 ([https://github.com/immunogenomics/HLA\\_analyses\\_tutorial](https://github.com/immunogenomics/HLA_analyses_tutorial)). Definitions of key terms used  
102 throughout this article can be found in **Box 1**.

103

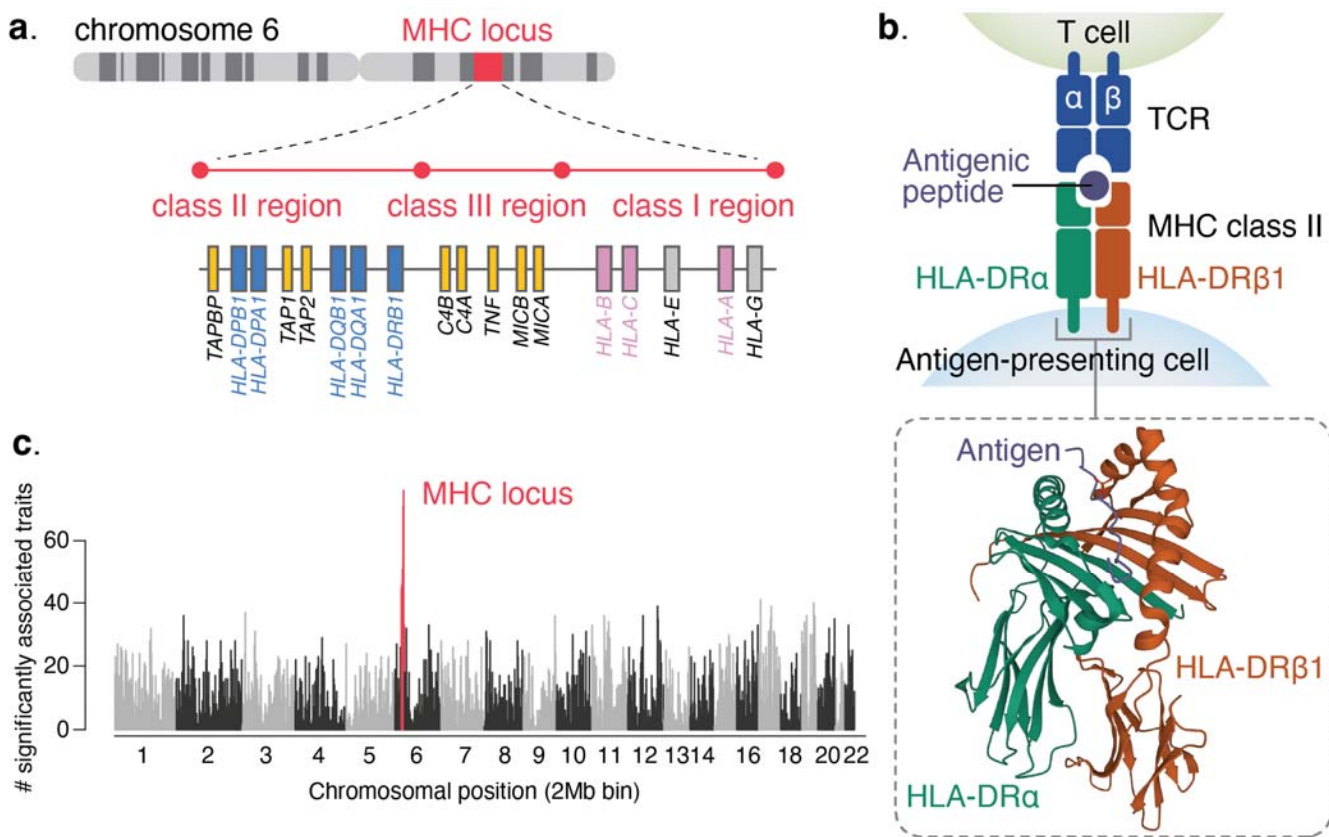
## Box 1 Key terms and definitions

---

MHC region	A genomic region that harbors the major histocompatibility complex (MHC). In GRCh37, it corresponds to chr6:28,477,797-33,448,354 (6p22.1-21.3).
Linkage disequilibrium	A non-random association or dependence of alleles at different loci in a given population, making the frequencies of the alleles deviate from the expected when the alleles were independent.
Imputation	A procedure of estimating the missing genotypes at loci that are not assayed in the target dataset.
Reference panel	A panel of densely genotyped haplotypes to be referred to when predicting the missing genotypes in the target cohort through imputation.
Haplotype	A stretch of DNA sequences (including multiple polymorphic loci) along one chromosome that tend to be inherited together due to linkage disequilibrium.
Allele	One of two versions of DNA sequences. An individual inherits two alleles (maternal and paternal) for any genomic location.
HLA allele	One of the sequence variations at a given <i>HLA</i> gene.
Genotype	An individual's pattern of DNA sequence at a given location. Two alleles from a mother and a father comprise a genotype.
Fine-mapping	A procedure to narrow down and define potentially causal genetic variation(s) affecting the trait of interest, from all the associated genetic variations at a given locus in GWAS by using statistical methods.
Homozygous	A state where the two alleles at the genetic variation of interest (e.g., an <i>HLA</i> gene) are the same.
Heterozygous	A state where the two alleles at the genetic variation of interest (e.g., an <i>HLA</i> gene) are different.
Allele divergence	A proxy for the functional difference in antigen binding between two HLA alleles based on the divergence of their amino acid sequence.

---

Sakaue et al.



106  
107 **Figure 1. A simplified summary of the location and structure of *HLA* genes on human**  
108 **chromosome 6, and their associations with human traits**

109 **a.** A schematic representation of the human MHC locus, three classes of the region, and genes  
110 within them. The genes in pink are the classical class I *HLA* genes, whereas those in blue are  
111 the classical class II *HLA* genes. **b.** Presentation of antigenic peptide by an antigen-presenting  
112 cell to a T cell through interaction between MHC class II molecule and T cell receptor (TCR).  
113 The inset describes protein structure of MHC class II, HLA-DRA and DRB1 adapted from PDB  
114 (3L6F). **c.** The number of traits associated with any variants within 2Mb genomic window with  $P$   
115  $< 5 \times 10^{-8}$  in UK Biobank or meta-analysis of UK Biobank and FinnGen among 198 diseases and  
116 biomarkers<sup>9</sup>.

Sakaue et al.

117 *Summary of the protocol*

118 The protocol is summarized in **Figure 2a**. The protocol is comprised of two sections: HLA  
119 imputation (**Figure 2a-1**) and HLA association testing (**Figure 2a-2**). HLA imputation is a  
120 method to infer HLA alleles, amino acids and SNPs from microarray-based genotype within the  
121 MHC region. We first introduce the concept of the HLA reference panel (1), which is used as a  
122 dictionary to search for similar haplotypes (keyword) to infer unknown HLA types (definition).  
123 We highlight specifically our multi-ancestry HLA reference panel, which we recently constructed  
124 to enable accurate HLA inference in diverse global populations<sup>10</sup>. We next provide specific  
125 instructions to perform QC of the input genotype data (2), per-individual and per-variant (3). The  
126 quality of genotype data is critical in achieving accurate imputation, and a special caution  
127 should be taken given the extremely complex and polymorphic nature of genetic variants within  
128 MHC. We then introduce options to impute HLA (4), either (i) on a user's local server or (ii) or by  
129 using the Michigan Imputation Server (MIS)<sup>11</sup>, which is a publicly available, web-based  
130 imputation platform we jointly support with Michigan University. We finally describe the quality  
131 metrics and post QC of the imputed variants (5).

132 We next describe statistical methods to perform comprehensive association tests between  
133 HLA genotype and human traits (**Figure 2a-2**). Since HLA associations are often explained by  
134 amino acid sequences in the peptide binding groove of HLA molecules<sup>12</sup>, we describe  
135 strategies to fine-map associations with the aim of pinpointing causal variation. We start from a  
136 simple single-marker test which is similar to that commonly used in GWAS, and then elaborate  
137 on the HLA-specific fine-mapping methods (e.g., an omnibus test (2) and a conditional

Sakaue et al.

138 haplotype test (3)). We also introduce statistical tests to define non-additive, interactive, and  
139 multi-trait contribution of HLA alleles.  
140

Sakaue et al.

**a. a-1. HLA imputation**

**(1) The HLA imputation reference panel**

Scaffold genotype in the MHC HLA alleles HLA amino acids HLA intragenic SNPs  
 CGAGATCTCAGTCTCTGTTCTAA DRB1\*04:01 GGSCMAALTVTLMVL GGAGGACCTGTGAACCA  
 CAAGATTCTCTCATCTGTTCTAA DRB1\*01:01 GGSCMTALTVTLMVL GGAAGACCTGCGAACCA  
 CGAGATCTCCTGCTCAGTCTAA DRB1\*01:02 GGSCMTALTVTLMVL GGAGGACCTGTGAACCA  
 CAAGATCTCCGCTCTGTTCTAA DRB1\*15:01 GGSCMTALTVTLMVL GGAAGACCTGTGAACCG

**(2) Input from the target cohort**

Genotype in the MHC region  
 CGA.ATCT..GTCTCTGT.CTAA [?][?][?]  
 CAA.ATCT..GTCT.TGT.CTAA [?][?][?]  
 CAA.ATT..TGTTCACT.CTAA [?][?][?]

**(3) Quality control → (4) Phasing + Imputation**

- Per-sample
- SNP2HLA
- Per-variant
- Michigan Imputation Server (MIS)

**(5) Output of HLA imputation for the target cohort**

CGAGATCTCAGTCTCTGTTCTAA DRB1\*04:01 GGSCMAALTVTLMVL GGAGGACCTGTGAACCA  
 CAAGATCTCCGCTCTGTTCTAA DRB1\*15:01 GGSCMTALTVTLMVL GGAAGACCTGTGAACCG  
 CAAGATTCTGCTCAGTCTAA DRB1\*01:01 GGSCMTALTVTLMVL GGAAGACCTGCGAACCA

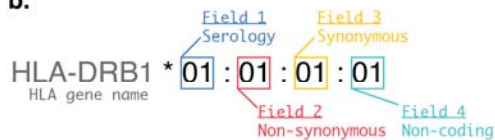
**a-2. HLA association and fine-mapping**

Disease ↔ (1) HLA alleles (2) HLA amino acid positions (Omnibus test)

HLA-DRB1\*01:01 GGSCMAALTVTLMVLSSP  
 HLA-DRB1\*04:01 GGSCMTALTVTLMVLSSP  
 HLA-DRB1\*15:01 GGSCMTALTVTLMVLS

(3) HLA haplotypes (Conditional haplotype test)

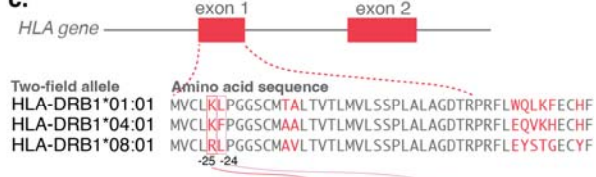
**b.**



Alleles

One-field allele	HLA-DRB1*01
Two-field allele	HLA-DRB1*01:01
Three-field allele	HLA-DRB1*01:01:01
Four-field allele	HLA-DRB1*01:01:01:01
G-group allele	HLA-DRB1*01:01:01G
P-group allele	HLA-DRB1*01:01P

**c.**



Two-field allele	HLA-DRB1*01:01	HLA-DRB1*04:01	HLA-DRB1*08:01
Amino acid sequence	MVCL <b>K</b> LPGGSCM <b>A</b> LTVTLMVLSSPLALAGDTRPRFL <b>W</b> QLK <b>F</b> CHF	MVCL <b>K</b> LP <b>F</b> PGGSCM <b>A</b> LTVTLMVLSSPLALAGDTRPRFL <b>E</b> QV <b>K</b> HECHF	MVCL <b>R</b> LP <b>F</b> GGSCM <b>A</b> LTVTLMVLSSPLALAGDTRPRFL <b>E</b> Y <b>S</b> T <b>G</b> CF

-25 -24							
	DRB1*01:01	04:01	08:01	-25_K	-25_R	-24_L	-24_F
	1	0	0	1	0	1	0
	Haplotype_A	Haplotype_B	Haplotype_C				
	0	1	0	1	0	0	1
	Haplotype_A	Haplotype_B	Haplotype_C				
	0	0	1	0	1	1	0

141

142 **Figure 2. The overview of HLA imputation, association, and fine-mapping, including**  
 143 **construction of HLA reference panel.**

144 **a.** Overview of this protocol. **(a-1)** A toy example of HLA imputation, describing (1) HLA  
 145 imputation reference panel, (2) input genotype in the MHC region from the target cohort without  
 146 HLA types, (3) quality control of the target genotype, (4) genotype phasing and imputation to  
 147 predict the untyped HLA alleles in the target cohort, and (5) output of the predicted HLA alleles.

148 **(a-2)** Statistical methods to investigate and fine-map association of HLA alleles, amino acids  
 149 and their haplotypes with a trait of interest. **b.** The naming system (nomenclature) of HLA alleles,  
 150 consisting of four fields with each field corresponding to the types and consequences of  
 151 nucleotide variations. **c.** (top) The amino acid sequences defining each of three example  
 152 HLA-DRB1 alleles. The amino acids colored in red indicate the positions where they have  
 153 variations among the alleles. The numbers (-25 and -24) at the bottom indicate the relative  
 154 position of those amino acids within a coding region of HLA-DRB1. (bottom) A procedure to

Sakaue et al.

155 code each of the HLA alleles and amino acid polymorphisms as binary markers: 1 if that marker  
156 is present within a haplotype and 0 otherwise. Each of the residues are coded separately for a  
157 given amino acid position in the corresponding HLA protein.

158

159

Sakaue et al.

160 *Introduction to HLA nomenclature*

161 Sequence variation within *HLA* genes is organized by the International Immunogenetics  
162 database (IMGT)<sup>13</sup>, which has documented and named 33,490 unique *HLA* alleles (URL:  
163 <https://www.ebi.ac.uk/ipd/imgt/hla/about/statistics/>). Within each of the *HLA* alleles, there are  
164 nucleotide variants which sometimes cause amino acid changes (i.e., non-synonymous  
165 nucleotide substitutions) and sometimes not (i.e., synonymous, intronic and intergenic  
166 nucleotide substitutions). A detailed nomenclature system at IMGT has been developed to  
167 organize those polymorphisms in *HLA* genes into four fields (**Figure 2b**)<sup>14</sup>. In this nomenclature,  
168 field 1 (i.e., the first two digits, e.g., HLA-DRB1\*01) describes the serological type, which was  
169 historically defined based on similar seroreactivity to immunological reagents. Field 2 (i.e., the  
170 next set of digits, e.g., HLA-DRB1\*01:01) corresponds to the unique amino acid sequence of  
171 the gene; all the non-synonymous changes are reflected in this set. Field 3 (e.g.,  
172 HLA-DRB1\*01:01:01) reflects synonymous nucleotide substitutions within the coding  
173 sequences, and field 4 (e.g., HLA-DRB1\*01:01:01:01) reflects polymorphisms within the  
174 intronic or non-coding regions. Thus, whereas nucleotide variants define *HLA* alleles at up to  
175 four-field resolution, most disease associations are captured by two-field *HLA* resolution since  
176 amino acid sequence captures most of the structural differences between the alleles.

177 The four-field naming system is the current standard and most widely used, but it is worth  
178 expanding upon the alternative nomenclatures since they are sometimes seen in practice.  
179 Before the current four-field naming system was introduced, the IMGT had used the  
180 nomenclature without a field separator (':'), where each field must have two digits. Therefore,

Sakaue et al.

181 one-field alleles had been called two-digit alleles, and two-field alleles had been called four-digit  
182 alleles. However, as the number of two-field alleles belonging to a given one-field allele began  
183 to exceed 100 (e.g., HLA-A\*02101 and HLA-B\*15101), the name “four-digit” designation  
184 became inappropriate. Thus, the IMGT updated the previous nomenclature system by  
185 introducing the field separator (e.g., HLA-A\*02:101 and HLA-B\*15:101) and four-field naming  
186 system.

187 In this same update, the IMGT introduced two additional nomenclature schemes to  
188 facilitate practical reporting of HLA typing: G group and P group. Current classical HLA typing  
189 technologies sometimes cannot resolve an HLA allele at four-field resolution and define a group  
190 of similar alleles based on the variations within peptide binding domains (exon 2 and 3 for class  
191 I HLA genes and exon 2 for class II HLA genes). The G group nomenclature represents HLA  
192 alleles that share the same nucleotide sequence in the peptide binding domains. For instance,  
193 HLA-A\*01:02:01G includes HLA-A\*01:02:01:01, HLA-A\*01:02:01:02, HLA-A\*01:02:01:03, and  
194 HLA-A\*01:412, but not HLA-A\*01:02:02. The P group nomenclature represents HLA alleles that  
195 share the same protein sequence in the peptide binding domains. For example, HLA-A\*01:02P  
196 includes HLA-A\*01:02:01:01, HLA-A\*01:02:01:02, HLA-A\*01:02:01:03, HLA-A\*01:02:02, and  
197 HLA-A\*01:412.

198

199 *Introduction to HLA imputation*

200 Genotype imputation is the term used to describe estimation of missing genotypes that are not  
201 assayed in the target dataset. Most imputation methods use data from densely genotyped

Sakaue et al.

202 samples as a reference dataset in which haplotypes have been inferred<sup>15</sup>. They typically use  
203 statistical approaches such as hidden Markov models (HMM) to fill in missing genotypes in a  
204 dataset of interest with incomplete genotype data. Here the genotype data reflects the observed  
205 states, while the template haplotypes are represented as the unknown hidden states. Most  
206 imputation algorithms produce a probabilistic prediction of each imputed genotype. These  
207 probabilities can be used to either (1) calculate a probabilistic dosage, which is a simple sum of  
208 those expected probabilistic allele count, or (2) a best-guess genotype, which is a combination  
209 of alleles which have the largest probability. These values can then be used in the downstream  
210 analyses. Dosages inferred from imputed results are a continuous value between 0 and 2,  
211 whereas guess genotypes are discrete values of 0, 1, or 2 alleles. Genotype imputation can  
212 boost the power of the association studies, fine-map the signal, and enable meta-analysis of  
213 multiple cohorts<sup>15</sup>.

214 After imputation, it is essential to understand the accuracy of imputation. The quality of  
215 predictions can be technically measured by masking the genotype, imputing them, and deriving  
216 the correlation between the true (masked) genotype and the predicted genotype. We favor  
217 using this correlation as a metric, as opposed to accuracy (percent of concordance between  
218 true genotype and imputed genotype calls), since accuracy can be upwardly biased for rare  
219 alleles. In practice, true genotype data is often missing. In these instances, we can also  
220 estimate the quality of imputation by the ratio of the empirically observed variance of the allele  
221 dosage to the expected binomial variance at Hardy-Weinberg equilibrium ( $R_{sq}$ ).

Sakaue et al.

222 HLA imputation is natural extension of the genotype imputation. The HLA imputation infers  
223 HLA alleles, amino acid polymorphisms, and intragenic SNPs within *HLA* (hidden state). Due to  
224 the excessive variation of these *HLA* genes, these variants generally cannot be accurately  
225 assayed with popular probe-based genotyping arrays. HLA alleles are inferred indirectly by  
226 using surrounding genotyped SNP variants in the MHC region (“scaffold” variants; **Figure 2c**).  
227 Reference haplotypes are constructed from samples with both genotyped SNP variants and  
228 HLA alleles genotyped by either classical sequence-based typing (SBT)<sup>16</sup> or inference from  
229 untargeted sequencing data, such as whole genome sequencing (WGS) data<sup>17,18</sup>. The HLA  
230 amino acid sequences and intragenic SNPs within *HLA* genes can also be included in the  
231 reference haplotypes to enable their imputation. There are many widely used statistical  
232 software tools to perform the HLA imputation, such as SNP2HLA<sup>19</sup>, HIBAG<sup>20</sup>, and HLA\*IMP<sup>21</sup>,  
233 HLA-IMPUTER<sup>22</sup>, and GRIMM<sup>23</sup>. The SNP2HLA and HLA\*IMP methods use the same HMM  
234 algorithm used in genome-wide imputation, whereas the HIBAG method uses a  
235 machine-learning technique: a bagging method<sup>24</sup>. Imputation performance is often related to  
236 the size, quality, and suitability of the reference panel rather than the statistical software used.  
237 The output of the HLA imputation is a posterior probability as well as an effective dosage  
238 (ranging from 0 to 2) for each HLA allele in a given sample. Subsequent association tests  
239 usually account for the uncertainty of the imputation by using the estimated dosage as an  
240 explanatory variable.  
241  
242 *HLA imputation reference panel*

Sakaue et al.

243 There have been many efforts to construct haplotype reference panels in the MHC region to  
244 enable HLA imputation. Since the haplotype structure within the MHC region differs significantly  
245 among populations<sup>10</sup>, it is important that the target dataset is well represented by the reference  
246 haplotype panel. The current availability of published HLA reference panels is summarized in  
247 **Table 1**.

Sakaue et al.

Imputation software	Name	Ancestry/population	N <sub>samples</sub>	Availability
SNP2HLA <sup>19</sup>	T1DGC	European	5,225	Upon registration
SNP2HLA	Pan Asian <sup>25</sup>	Han Chinese, Southeast Asian Malay, Tamil Indian ancestries, and Japanese	530	Publicly available
SNP2HLA	Hirata et al. <sup>26</sup>	Japanese	1,120	Upon request
SNP2HLA	Zhou et al. <sup>27</sup>	Han Chinese	20,635	Publicly available
SNP2HLA	Kim et al. <sup>28</sup>	Korean	413	Publicly available
SNP2HLA HLA-TAPAS <sup>1</sup> 0	1KG	Global populations in 1000 Genomes Project	2,504	Publicly available
	1KG	Global populations in 1000 Genomes Project	2,504	Publicly available
MIS (Minimac)	Multi-ancestry	Multi-ancestry	20,349	Limited public accessibility on web
HIBAG <sup>20</sup>	HLARES	Multi-ancestry	4,000	Publicly available
HIBAG	IKMB Degenhardt et al. 1958 Birth Cohort +	Multi-ancestry	1,360	Publicly available
HIBAG	HapMapCEU	European	~1,300	Upon request
HLA*IMP <sup>21</sup>			~2,500	Limited public accessibility on web

248 **Table 1. A list of available HLA imputation reference panels**

249 A list of currently available HLA imputation reference panels, the sample ancestry, the number  
250 of samples, and whether they are publicly available or not. Limited public accessibility means  
251 that while the raw reference panel (individual-level genetic data) is not accessible, users can  
252 use it for imputation via web-based imputation service. MIS: Michigan Imputation Server.

253

254

255

Sakaue et al.

256 It is also possible to construct a custom HLA reference panel. SNP2HLA and  
257 HLA-TAPAS<sup>10,19</sup> are tools to construct such custom reference panels. Starting with a SNP  
258 genotyped cohort (“scaffold variants”), we can either (1) obtain the gold standard SBT of HLA  
259 alleles (such as sequence-specific oligonucleotide probe hybridization (SSOP)<sup>16</sup>) if DNA is  
260 available or (2) infer HLA alleles from WGS (e.g., HLA\*PRG and HLA\*LA)<sup>17,18,29</sup>. Reference  
261 panels can include alleles of classical *HLA* genes ( $n_{\text{gene}} = 8$ )<sup>10</sup>, which are most polymorphic and  
262 disease-associated, or both classical and non-classical *HLA* genes ( $n_{\text{gene}} = 33$ )<sup>26</sup>. In the  
263 SNP2HLA algorithm, HLA alleles are converted to biallelic markers (e.g., 1 indicates the  
264 presence of the allele and 0 indicates the absence of the allele). Classical SBT, such as SSOP,  
265 is the most accurate approach to HLA genotyping. Incorporation of SBT genotypes into  
266 reference panels results in highly accurate imputation; however, since SBT is costly and  
267 labor-intensive, it cannot be easily used to build large reference panels. Graph-based inference  
268 of HLA alleles from WGS is a potential alternative method that can be easily applied to large  
269 sequencing datasets that are increasingly available<sup>17,18,29</sup>. However, an important caveat is that  
270 the accuracy of HLA typing by those graph-based methods can be variable. For example,  
271 imputation performance is affected by (i) quality of the sequencing data, (ii) read depth and  
272 length, (iii) representation of the population in reference databases such as IMGT, and (iv) the  
273 degree of sequence variation within the targeted *HLA* gene. For studying under-represented  
274 populations or highly polymorphic genes, gold standard SSOP might still be necessary to  
275 construct a suitably accurate reference panel.

Sakaue et al.

276 To enable imputation of amino acid polymorphisms and intragenic HLA SNPs, we can  
277 encode all these variants as binary markers based on the reference amino acid and nucleotide  
278 sequences of each observed HLA allele from the IMGT HLA Database  
279 (<https://www.ebi.ac.uk/ipd/imgt/hla/>) (**Figure 2d**). The scaffold genetic variants within the MHC  
280 region are usually obtained by either genotyping with a SNP microarray or WGS. Stringent SNP  
281 QC is essential for accurate phasing, and ultimately accurate imputation. In constructing and  
282 updating a multi-ancestry HLA reference panel, we optimized this QC process to maximize  
283 imputation accuracy. Specifically, we started with QCing each of the global cohorts separately,  
284 with genotype call rate (> 95%) and sample call rate (>90%). We then retained all the variants  
285 that were present in the 1000 Genomes Project and excluded any variants that were not  
286 included in commonly used genotyping arrays (Illumina Multi-Ethnic Genotyping Array, Global  
287 Screening Array, OmniExpressExome, and Human Core Exome), since these variants that are  
288 not included in the target genotype data are more likely to result in phasing switch errors without  
289 improving imputation accuracy. When combining all the cohorts to construct the multi-ancestry  
290 panel, we cross-imputed all the variants together to avoid excluding population-specific variants  
291 that are polymorphic in a specific cohort but monomorphic and thus not called in the other  
292 cohorts (**Supplementary Figure 1**). The final reference panel includes the HLA alleles, amino  
293 acids, intragenic HLA SNPs, and the “scaffold” variants (i.e., SNP variants outside of *HLA* gene  
294 but within the extended MHC region), which are then phased statistically or by using trios.  
295 Imputed HLA alleles and variants are often used for subsequent association testing and  
296 meta-analyses to fine-map disease risk. Such studies potentially include data from multiple

Sakaue et al.

297 cohorts, datasets, or populations. To avoid spurious associations due to batch effects and  
298 population stratification, it is essential to perform HLA imputation on all datasets using the same  
299 reference panel, ideally with all case and control samples genotyped together. Given that such  
300 case-control cohorts may originate from multiple populations to increase the fine-mapping  
301 resolution, we previously constructed an HLA reference panel covering multiple global  
302 populations<sup>10</sup>.

303 With the publication of this protocol, we present an updated version of this multi-ancestry  
304 panel (version 2). Briefly, we added samples from European ( $n = 2,233$ ) and Japanese ( $n =$   
305 723) ancestry for a total of 20,349 individuals. This panel represents admixed African, East  
306 Asian, European and Latino populations. We also updated HLA allele calls and a set of scaffold  
307 variants. We plan to maintain and update the panel further to increase representation of globally  
308 diverse populations, improve the HLA allele calls, and refine selection of the scaffold variants to  
309 achieve the most accurate imputation.

310

#### 311 *Recommendations for collecting genotype and phenotype information*

312 When designing a study to investigate the effect of HLA variation on human traits, it is important  
313 to be strategic when collecting genotype and phenotype data. For genotype data collection, one  
314 should ensure that the genotyping array used for the target cohort has a high coverage in the  
315 MHC region in order to adequately tag, through LD, HLA alleles, which contributes to accurate  
316 imputation. While most currently used genotyping arrays include a sufficient number of SNPs to  
317 tag HLA alleles for accurate imputation, some arrays have limited SNP coverage of the MHC

Sakaue et al.

318 region (**Supplementary Table 1**)<sup>30</sup>. We and others have shown that lower MHC coverage  
319 results in inaccurate imputation<sup>19,31</sup>. Furthermore, all study participants should ideally be  
320 genotyped together with the same genotyping array, to avoid introducing any structure that  
321 could cause a bias in imputation and the subsequent association testing and possibly  
322 fine-mapping.

323 Careful phenotype curation is very important when fine-mapping disease-associated  
324 variants. Discovery of HLA association signals can be enhanced by the addition of more  
325 samples, even at the risk of misclassified samples. However, fine-mapping can be affected by  
326 including misclassified samples. For example, studies of autoimmune disease including  
327 individuals with different subgroups of patients can obscure efforts to localize disease alleles.  
328 This has for instance been observed in rheumatoid arthritis, where patients with positive  
329 antibody status are phenotypically and genetically different from those with negative antibody  
330 status<sup>32,33</sup>. Recently, many efforts have been made to curate the phenotypes in large-scale  
331 biobanks<sup>34</sup> using self-reported disease status or billing code (e.g., ICD-10)<sup>35</sup>. While the total  
332 number of samples with these forms of phenotyping is large in these biobanks and may enable  
333 discovery, imprecise phenotype labeling may confuse HLA fine-mapping. In contrast,  
334 physician-curated cohorts may be important for fine-mapping efforts.

335 In addition to disease phenotypes, one must exercise caution when measuring HLA-related  
336 molecular phenotypes, such as *HLA* gene and protein expression. It is well established that  
337 HLA gene and protein expression is affected by the *cis*-regulatory genetic variants (i.e.,  
338 expression quantitative trait loci (eQTL) and protein expression quantitative trait loci

Sakaue et al.

339 (pQTL))<sup>36–38</sup>. When conducting eQTL studies, measuring *HLA* expression in RNA-seq is  
340 particularly challenging due to the high degree of genetic polymorphism among individuals.  
341 Standard expression quantification pipelines rely on a single human reference genome to align  
342 sequencing reads. The number of reads mapping to each *HLA* gene might be biased for two  
343 reasons: (1) the reads may fail to map to the reference due to the high degree of sequence  
344 variation (i.e., a large number of mismatches) and (2) the reads may not uniquely map to a  
345 single gene in the reference due to the similarity among nearby *HLA* genes (i.e.,  
346 multi-mapping)<sup>38</sup>. To address this, more accurate gene expression estimates can be obtained  
347 by using an HLA-personalized reference<sup>38</sup>; instead of using a standard single human reference  
348 genome, we can supply customized HLA sequences for each target individual for each *HLA*  
349 gene (either based on classical HLA typing or HLA imputation) to minimize the degree of  
350 variation between the RNA-seq reads and the reference and hence reduce the possibility of  
351 mapping failures and multi-mapping. Similarly, caution should be taken for HLA pQTL studies.  
352 HLA protein expression is often measured by antibody-based methods (e.g., antibody-derived  
353 tags) at single-cell resolution. However, these antibodies may have differing binding affinities to  
354 the protein products of different HLA alleles. We should take caution when conducting pQTL  
355 studies, since this differing affinity might cause a bias towards specific HLA alleles when  
356 measuring the abundance of HLA proteins across individuals.

357

358 *Quality control of the target genotype data*

Sakaue et al.

359 Data quality control (QC) of genotype data prior to HLA imputation is extremely important. We  
360 next outline the basic QC measures commonly used in GWAS<sup>39</sup>, as well as specific instructions  
361 to handle genetic variants within the MHC region. These QC measures are typically performed  
362 once for each genotyping batch, followed by data integration and the final QC for the combined  
363 dataset (**Figure 3**).

364

### 365 **Per-individual QC**

366 We follow established guidelines<sup>34,39,40</sup> to perform standard per-individual QC in GWAS.  
367 Typically, we remove (i) individuals with high missingness (e.g., > 0.02), (ii) individuals with  
368 outlier high heterozygosity on suspicion of sample contamination, (iii) individuals with  
369 discordant sex information between the meta data and genotype, and (iv) individuals suspected  
370 to be duplicate samples based on genotype relatedness. We note that the threshold for each  
371 QC measure could be data-dependent, and thus we recommend reviewing the distributions of  
372 those metrics for each of the datasets.

373

### 374 **Per-variant QC**

375 It is important to select high-quality variants to achieve accurate imputation. We will describe  
376 the variant QC that is generally recommended for GWAS as well as specific considerations for  
377 the MHC region. As part of standard GWAS QC, we recommend ensuring that the target  
378 genotype data has genomic positions based on the same genome build as the reference panel.  
379 LiftOver software<sup>41</sup> can be used to lift the genomic position over to the desired genome build.

Sakaue et al.

380 Next, genomic variants are typically aligned to the forward strand to be consistent with the  
381 reference panel. We also identify duplicated variants within the dataset based on genomic  
382 position and alleles, and de-duplicate them by removing ones with higher missingness. We then  
383 remove (i) variants with high missingness (e.g., > 0.01), (ii) variants demonstrating a significant  
384 deviation from the Hardy-Weinberg equilibrium (HWE), and (iii) variants with very low minor  
385 allele frequency (MAF). Specifically, we remove variants with very low MAF (e.g., < 0.01 or  
386 0.005) or small minor allele count (MAC; e.g., < 5), assuming low accuracy in genotype calling  
387 from clustering. The sample size and the estimated ancestry should be accounted for when  
388 selecting the threshold in order to retain informative population-specific markers. We usually  
389 only keep biallelic variants and remove multi-allelic variants for simplicity in the imputation.

390 Specific caution should also be taken for per-variant QC in the MHC region, due to (i) highly  
391 variable allele frequency (AF) of variants within MHC across populations and (ii) expected HWE  
392 deviation in the MHC variants due to natural selection. For example, we usually align target  
393 genotype alleles to the forward strand. For non-palindromic SNPs (i.e., SNPs without A/T or  
394 G/C allele combinations), it is easy to do so by looking up the alleles with the same position in  
395 the reference human genome sequence on forward strand. If the alleles between the target and  
396 the reference genome are different (e.g., A/C in the reference but T/G in the target), we flip the  
397 alleles in the target dataset (swap alleles from T to A and from G to C in the target). On the  
398 other hand, in handling palindromic SNPs (i.e., SNPs with A/T or G/C alleles), we usually  
399 compare population-derived AF and the AF in the target dataset to eliminate allele ambiguity. If  
400 the AFs between them are largely different (e.g., A: 20% and T: 80% in the population reference

Sakaue et al.

401 but A: 78% and T: 22% in the target), we can flip the alleles to be consistent with the  
402 population-derived AF (swap alleles from A to T and from T to A in the target). However, this  
403 strategy might be ineffective within the MHC since reference AF for those SNPs might be  
404 different from the target samples when the study population is different, when there are large  
405 AF differences between cases and controls in case-control studies, or when the study sample  
406 size is too small to estimate AF accurately. Therefore, when the strand information of those  
407 palindromic SNPs is ambiguous in the target genotyping array or the genotyped data, it may be  
408 preferable to exclude all the palindromic SNPs. Second, we may compare AF of the variants  
409 after QC in the target data with AF in the population-frequency database (e.g., 1000 Genomes  
410 Project<sup>42</sup> and gnomAD<sup>43</sup>) or AF in the reference panel as a sanity check. When the AFs are very  
411 different between the two, those variants could be subject to genotyping error and should  
412 probably be removed. However, when the population does not exactly match between the  
413 target and the database or the reference, this strategy might be ineffective within the MHC.  
414 Thus, we could consider using a liberal threshold when removing variants based on the AF  
415 differences. Third, the extreme deviation from HWE is usually indicative of a genotyping or  
416 genotype-calling error that results in poor clustering<sup>44–46</sup> and is used as a metric to exclude poor  
417 quality variants. However, the deviation from HWE is to some extent expected in the MHC  
418 region due to natural selection<sup>47</sup> or due to the difference in allele frequency between cases and  
419 controls. The expected deviation will be greater when we study a cohort from multiple  
420 populations or of admixed ancestry, or when the effect size of HLA on the disease is large.  
421 Therefore, for the purpose of per-variant QC, we could consider (1) calculating HWE *P* values

Sakaue et al.

422 only within control individuals (as is generally recommended in GWAS), (2) calculating HWE  $P$   
423 values within individuals from a representative single-ancestry, or (3) using liberal threshold  
424 such as HWE  $P < 1 \times 10^{-10}$  when removing the variants suspected of poor clustering while  
425 retaining the important markers for HLA imputation. When we are unsure about the threshold,  
426 an appropriate value can be identified by visually inspecting the genotype cluster plots.

427

428 *Tools for genotype phasing and HLA imputation*

429 Once we QC the target genotype data and prepare the optimal HLA reference panel, we start  
430 HLA imputation for the target data using existing tools. **Table 2** summarizes the main software  
431 programs for HLA imputation and the available HLA reference panels. Of note, some imputation  
432 programs take as input the genotype files directly after the QC as described above, while others  
433 require users to pre-phase the genotypes to obtain haplotypes<sup>11,21</sup> before imputation (**Figure 3**).

434

435

Sakaue et al.

Imputation software	Pre-phasing	Input format	file Local	Output	Amino acid imputation
SNP2HLA <sup>19</sup>	Unnecessary	plink	Yes	VCF	Yes
SNP2HLA+Minimac	Necessary Recommended	phased VCF	Yes	VCF	Yes
MIS (Minimac)	when <i>N</i> is small	VCF	No	VCF R	Yes
HIBAG <sup>20</sup>	Unnecessary phased Oxford	plink	Yes	object	No
HLA*IMP <sup>21</sup>	Necessary	haps/sample	No	CSV	No

436 **Table 2. Representative software programs for HLA imputation and their requirements.**

437 A list of HLA imputation software programs and their specifications and details about the input  
438 and output. MIS: Michigan Imputation Server.

439

440

441

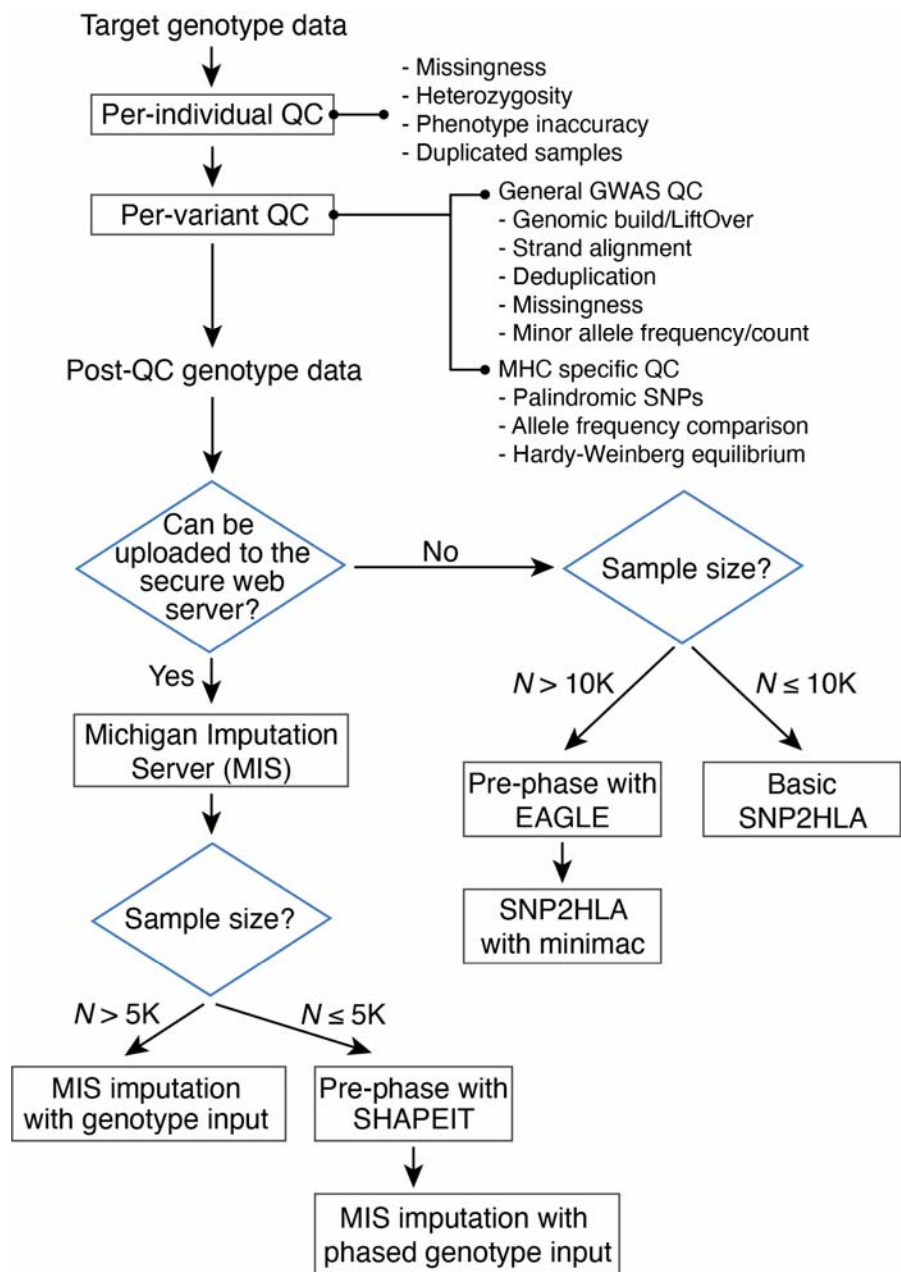
Sakaue et al.

442 Since our group has developed one of the most widely-used algorithms, SNP2HLA, and its  
443 extensions<sup>10,48</sup>, we will focus on the HLA imputation by using the SNP2HLA algorithm along  
444 with cloud based implementation at the MIS (URL:  
445 <https://imputationserver.sph.umich.edu/index.html>).

446

447

Sakaue et al.



448

449 **Figure 3. A flow chart of suggested analytical steps for genotype QC and HLA imputation**

450 A best-practice guideline to impute HLA alleles by using SNP2HLA algorithm, depending on the

451 characteristics of the target genotype data.

452

453

Sakaue et al.

454 **SNP2HLA**

455 The SNP2HLA<sup>19</sup> program can phase and impute HLA alleles, amino acids and intragenic SNPs  
456 with HMM implemented in BEAGLE<sup>49</sup> by taking the QCed target genotype file in the PLINK  
457 format as an input. The input file is internally processed to extract variants within the MHC (29  
458 Mb to 34 Mb), and then to correct or remove strand errors when possible based on genotype  
459 and AF of palindromic SNPs. In addition to the original bash scripts (URL:  
460 <http://software.broadinstitute.org/mpg/snp2hla/>), there are several extensions to the SNP2HLA  
461 algorithm such as HLA-TAPAS<sup>10</sup> and CookHLA<sup>48</sup>. We also provide a step-by-step explanation  
462 of the SNP2HLA implementation, along with a script that allows users to specify all the QC  
463 thresholds as option parameters to handle various target cohorts (e.g., the target populations,  
464 the number of samples, etc.) in our tutorial website  
465 ([https://github.com/immunogenomics/HLA\\_analyses\\_tutorial](https://github.com/immunogenomics/HLA_analyses_tutorial)).

466 We note that the original implementation using BEAGLE does not scale to a large number of  
467 samples in the target dataset, especially  $N > 10,000$ . To address this, we also provide a pipeline  
468 using the other representative imputation software, Minimac<sup>11</sup>, which can scale to hundreds of  
469 thousands to millions of individuals  
470 ([https://github.com/immunogenomics/HLA\\_analyses\\_tutorial](https://github.com/immunogenomics/HLA_analyses_tutorial)). To use Minimac for imputation,  
471 we first pre-phase the genotype by using methods such as SHAPEIT<sup>50</sup> or EAGLE<sup>51</sup>. EAGLE  
472 has an advantage of accurate and fast phasing when the number of samples is large (e.g.,  $N >$   
473 10,000). The pre-phased output file must be converted into the VCF format, and then used as  
474 an input to the Minimac software.

Sakaue et al.

475

476 **Michigan Imputation Server**

477 While HLA imputation using the SNP2HLA algorithm can be conducted locally using publicly  
478 available HLA reference panels, not all the HLA reference panels are available due to data  
479 sharing and privacy restrictions. Our latest multi-ancestry HLA reference panel is one such  
480 restricted-access panel<sup>10</sup>. To enable widespread access, we implemented HLA imputation on  
481 the Michigan Imputation Server (MIS; <https://imputationserver.sph.umich.edu/index.html>),  
482 which is a cloud-based imputation server with a user-friendly interface (**Supplementary Figure**  
483 **2**). We host the multi-ancestry HLA reference panel at the MIS and implement the HLA  
484 imputation using Minimac as described above. In brief, the user first creates an account online,  
485 and securely uploads either a phased or unphased VCF-format genotype file. If the uploaded  
486 genotypes are unphased, the uploaded genotype file will be phased within the MIS using the  
487 EAGLE algorithm. As noted above, we recommend to pre-phase the genotype (with the  
488 reference haplotype when possible) using SHAPEIT or other software when the sample size is  
489 small (e.g.,  $N < 5,000$ ) to achieve accurate phasing before imputation. The MIS automatically  
490 performs basic QC of the input VCF file for the strand orientation and alleles in accordance with  
491 the reference. If the input passes the QC steps, the MIS seamlessly performs the HLA  
492 imputation. The user will be notified with a download link for the imputed VCF file encrypted with  
493 a one-time password via an email once the imputation is completed. The MIS has been used to  
494 impute more than 6 million genomes since we started the web-based HLA imputation service in  
495 2021. We benchmarked the performance of HLA imputation on the MIS using individuals with

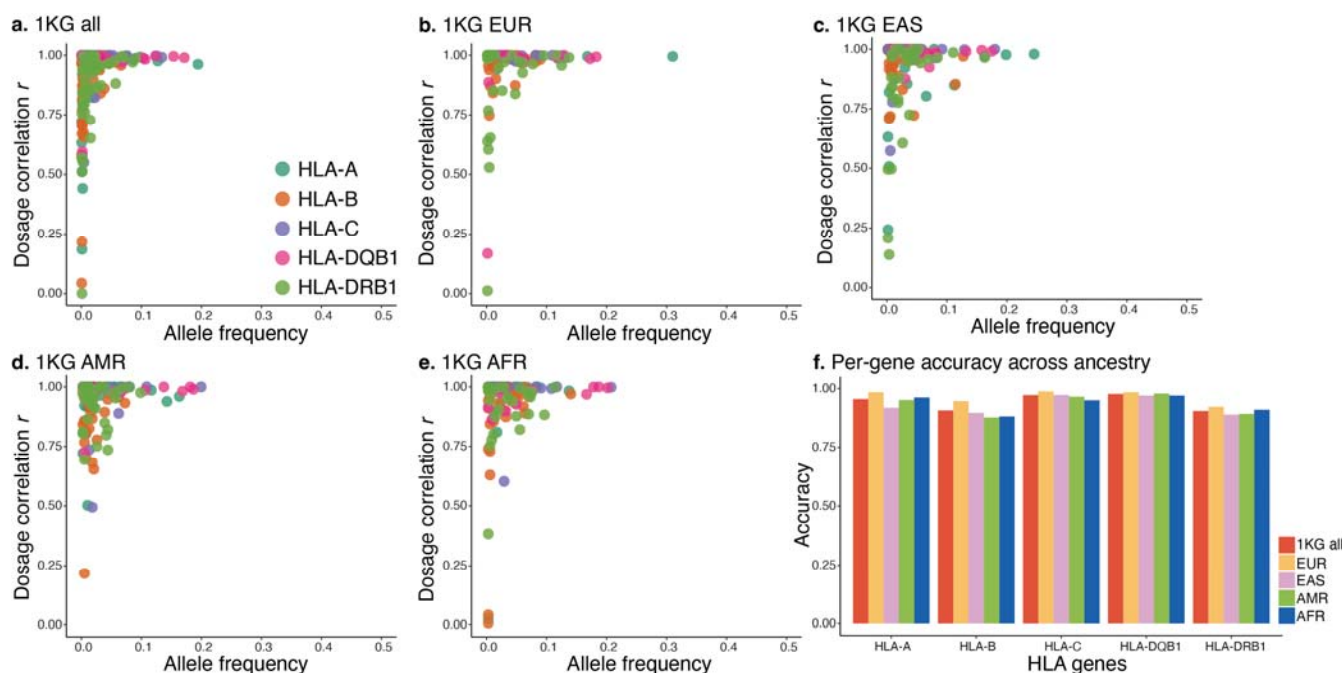
Sakaue et al.

496 both SNPs and (masked) gold-standard HLA alleles from the 1000 Genomes Project. We  
497 confirmed that the imputation accuracy measured by dosage correlation with true HLA alleles  
498 was very high across populations (mean dosage correlation  $r = 0.981$  for two-field alleles with  
499 MAF > 0.05; **Figure 4**).

500

501

Sakaue et al.



Sakaue et al.

512 *Post-imputation QC*

513 The output from the HLA imputation software is accompanied by a quality metric conveying the  
514 confidence or estimated accuracy of imputation per allele. A thorough review of these  
515 imputation metrics and their correspondence to imputation accuracy is described in Marchini  
516 and Howie<sup>15</sup>. We typically QC the imputed HLA alleles, amino acids, and intragenic SNPs  
517 based on imputation metrics before association testing. SNP2HLA, Minimac, and MIS all  
518 include *Rsq* as a quality metric. The appropriate *Rsq* threshold for QC may depend on the study  
519 design; for example, we commonly use *Rsq* > 0.7 in single cohort studies and *Rsq* > 0.5 in  
520 multi-cohort meta-analyses. By removing imputed alleles that are below this *Rsq* threshold,  
521 some individuals might end up having an *HLA* gene for which the total number of two-field  
522 alleles does not sum up to exactly 2. Those individuals might bias the fine-mapping of  
523 disease-causing alleles, which we will explain in the subsequent sections. Thus, we  
524 recommend removing any individuals that do not have two two-field alleles for a given gene  
525 when conducting conditional haplotype tests using two-field alleles.

526 We recommend calculating true imputation accuracy from classical HLA typing if it is  
527 available for a subset of study individuals. While the estimated imputation accuracy generally  
528 correlates well with the true accuracy, having the ability to internally benchmark with classical  
529 typing for a subset of the cohort is useful for evaluating the true imputation performance,  
530 especially if the reference panel imperfectly represents the genetic ancestry of the imputed  
531 cohort.

532

Sakaue et al.

533 *HLA association and fine-mapping*

534 **Single-marker tests**

535 Single-marker genetic association tests are used to investigate whether a specific HLA allele,  
536 amino acid or SNP is statistically associated with a risk of a disease or a trait of interest, such as  
537 risk for a given disease. Similar to the approach used in GWAS, we perform a logistic  
538 regression (for case-control traits) or a linear regression (for quantitative traits) for the imputed  
539 binary makers that indicate the presence (coded as T in the imputed VCF file) or absence  
540 (coded as A in the imputed VCF file) of the selected HLA allele, an amino acid, or an intragenic  
541 SNP. For the markers, we typically use the imputed probabilistic dosage genotypes to account  
542 for any imputation uncertainty. We include study-specific covariates that could independently  
543 explain the trait of interest, such as sex, age, and genotype batches, as well as genotype  
544 principal components (PCs) to account for population stratification and an indicator variable of  
545 cohorts when combining multiple cohorts.

546 The logistic regression can be formulated as:

$$\log(\text{odds}_i) = \beta_0 + \beta_a g_{a,i} + \sum_k \beta_k x_{k,i} + \sum_l \beta_l PC_{l,i}$$

547 where  $\log(\text{odds}_i)$  is the logged odds ratio for case-control status in individual  $i$ ,  $a$  indicates  
548 the specific allele being tested, and  $g_{a,i}$  is the imputed dosage of allele  $a$  in individual  $i$ . The  
549 allele  $a$  could be either HLA alleles, amino acid polymorphisms or SNPs. The  $\beta_a$  parameter  
550 represents the additive effect per allele. For all covariates  $k$ ,  $x_{k,i}$  and  $\beta_k$  are the covariate  $k$ 's  
551 value in individual  $i$  and the effect size for the covariate  $k$ , respectively. Similarly,  $PC_{l,i}$  and  $\beta_l$

Sakaue et al.

552 are the first  $l$ th genotype PC value in individual  $i$  and the effect size for the first  $l$ th genotype  
553 PC, respectively, to control for genetic ancestry. The  $\beta_0$  is the logistic regression intercept.

554 Quantitative traits that follow continuous distributions (e.g., antibody levels, blood cell counts  
555 etc.) can be analyzed by using linear regression similarly:

$$y = \beta_0 + \beta_a g_{a,i} + \sum_k \beta_k x_{k,i} + \sum_l \beta_l PC_{l,i}$$

556 where  $y$  is a quantitative trait of interest, and normalized by Z score or inverse-normal  
557 transformation when necessary.

558 These association tests can be conducted using conventional GWAS software, such as  
559 PLINK<sup>52</sup>, SAIGE<sup>53</sup>, BOLT<sup>54</sup>, etc. by directly using the output VCF files from either the SNP2HLA  
560 or the MIS. We use the dosage values designated as “DS” in the imputed VCF files to conduct  
561 dosage-based association tests. We provide example command-line scripts to perform single  
562 marker tests by using PLINK2 software at our website.

563 To interpret the results from such an association analysis, we ensure that the “effect allele”  
564 (i.e., the allele to which the effect estimate refers) is the presence (coded as P or T in  
565 SNP2HLA) of the allele. Also, we note that the association of rare alleles might be spurious due  
566 to both the limited accuracy in imputation and the noise in the estimate in the regression. Thus,  
567 we might QC the association statistics by MAF to exclude rare alleles (e.g., MAF < 1%). The  
568 odds ratio (OR) calculated from the beta ( $e^\beta$ ) is the estimated risk explained by having one copy  
569 of the HLA allele of interest, and the  $P$  value indicates its significance. Given the strength of LD  
570 in the MHC region, trait associations to multiple HLA alleles, amino acid polymorphisms or

Sakaue et al.

571 intragenic SNPs may yield significant results. Further analysis is then required to identify which  
572 allele(s) most significantly explains the disease risk within the HLA region.

573

574 **Omnibus tests for fine-mapping amino acid position**

575 To further narrow down the causal position within amino acid sequences within that *HLA* gene,  
576 we perform an omnibus test. This analysis is particularly useful when we seek to define  
577 mechanisms for the HLA association with the disease, for example by changing the amino-acid  
578 compositions at the peptide binding groove of the HLA molecule. In the omnibus test, we  
579 estimate the total effect on our trait of interest of all amino acid content variation at a given  
580 amino acid position, rather than the separate effects of individual amino acids that appear at  
581 that position, as we did in the single-marker test. For an amino acid position which has  $M$   
582 possible amino acid residues, we assess the significance of the improvement in fit for the full  
583 model which includes  $M - 1$  amino acid dosages as explanatory variables when compared to  
584 a reduced model without including those amino acid dosages. We usually select one amino  
585 acid residue that is most common in the studied cohort as the reference allele, and use all the  
586 other amino acid residues ( $M - 1$ ) as the explanatory variables. We assess the improvement in  
587 model fit by the delta deviance (sum of squares) using an F-test with  $M - 1$  degrees of  
588 freedom and derive the statistical significance of the improvement.

589 Full model:  $\log(\text{odds}_i) = \beta_0 + \sum_k \beta_k x_{k,i} + \sum_l \beta_l PC_{l,i} + \sum_{m=1}^{M-1} \beta_m AM_{m,i}$

590 Reduced model:  $\log(\text{odds}_i) = \beta_0 + \sum_k \beta_k x_{k,i} + \sum_l \beta_l PC_{l,i}$

Sakaue et al.

591 where  $m$  is one amino acid residue at this position,  $M$  is the total number of observed amino  
592 acid residues at this position,  $AM_{m,i}$  and  $\beta_m$  are the amino acid dosage of the residue  $m$  in  
593 individual  $i$  and the effect size for the residue  $m$ , respectively.

594 We may use the permutation procedure to determine whether the observed association at a  
595 single-marker test is primarily driven by HLA alleles (e.g, HLA-DRB1\*04:01) or amino acid  
596 polymorphisms (e.g., HLA-DR $\beta$ 1 positions 11, 71 and 74)<sup>12</sup>. To do so, we shuffle the  
597 correspondence between amino acid sequences and each of the two-field HLA alleles which  
598 was originally defined in IMGT database as described above, while preserving the relationship  
599 between the phenotype and the two-field HLA alleles. Then, in each permutation, we select  
600 each amino acid polymorphism and assess the improvement in deviance after including this  
601 amino acid polymorphism into the model. We typically perform  $> 10,000$  permutations. If the  
602 observed improvement using the actual data is significantly larger than the improvements using  
603 these permutations, we can infer that amino acid polymorphism is driving the signal, instead of  
604 observing the “synthetic” association driven by the HLA allele and its linkage with the causal  
605 amino acid(s).

606

## 607 **Conditional haplotype tests to define a risk sequence of amino acids**

608 Defining the exact stretches of HLA amino acid sequences driving the association with disease  
609 allows us to understand the mechanism by which amino acid change affects disease risk<sup>12</sup>.  
610 Importantly, to model combinations of positions, we must use phased genotyping information,  
611 rather than encoding each position separately. We perform a conditional haplotype test, where

Sakaue et al.

612 we utilize and combine the imputation results of both two-field alleles and amino acid  
613 polymorphisms to obtain phased information. Specifically, we start from the most significant  
614 position of amino acid sequence based on the omnibus test we described in the previous  
615 section. If there are  $M$  possible amino acid residues at this position, we can group all possible  
616 two-field alleles for this *HLA* gene into  $M$  groups based on the amino acid residue property at  
617 our selected position (**Figure 5a**). Recall that each two-field allele at a given *HLA* gene  
618 corresponds to a unique sequence of amino acids in this gene. In the same way as we did in the  
619 omnibus test based on the  $M$  amino acid residues, we can estimate the effect of each of the  $M$   
620 groups using a logistic regression model (including covariates, as described above) and derive  
621 the improvement in model fit over a reduced model without including those  $M$  groups.

622 Full model:  $\log(\text{odds}_i) = \beta_0 + \sum_k \beta_k x_{k,i} + \sum_l \beta_l PC_{l,i} + \sum_{m=1}^{M-1} \beta_m Gr_{m,i}$

623 Reduced model:  $\log(\text{odds}_i) = \beta_0 + \sum_k \beta_k x_{k,i} + \sum_l \beta_l PC_{l,i}$

624 where  $Gr_{m,i}$  is the sum of the dosage of two-field alleles from a group  $m$ , explained by the  
625  $m$ 'th amino acid residue. We note that we recommend removing any individuals that do not  
626 have two two-field alleles for a given gene, as we explained in the *Post-imputation QC* section.

627 Once we define the most significant individual position at a given *HLA* gene based on the  
628 significance of improvement, we next seek to identify which amino acid position other than this  
629 significant position best improves the model over the model only including this significant  
630 position (**Figure 5b**). Let  $x$  be the most significant position in the primary analysis, which has  
631  $X$  possible amino acid residues. We sequentially test each amino acid position ( $z$ ) other than  $x$ ,  
632 to ask whether haplotypes defined by the amino acid combination of positions  $x$  and  $z$  ( $z \neq x$ )

Sakaue et al.

633 explain the disease risk more than those defined only by the position  $x$ . To do so, we  
634 re-categorize all two-field alleles at this *HLA* gene into  $Z$  groups, where  $Z$  is the total number  
635 of observed haplotypes defined by the amino acid positions  $x$  and  $z$ . The value of  $Z$  must be  
636 at least  $X$  if no new haplotypes are defined. We again assess the significance of the  
637 improvement in model fit of the Full model (covariation at positions  $x$  and  $z$ ) over the Reduced  
638 model (variation at position  $x$  alone) by the delta deviance (sum of squares) using an F-test  
639 with  $Z - X$  degrees of freedom.

640 Full model:  $\log(\text{odds}_i) = \beta_0 + \sum_k \beta_k x_{k,i} + \sum_l \beta_l PC_{l,i} + \sum_{n=1}^{Z-1} \beta_{x+z,n} Gr_{x+z,n,i}$

641 Reduced model:  $\log(\text{odds}_i) = \beta_0 + \sum_k \beta_k x_{k,i} + \sum_l \beta_l PC_{l,i} + \sum_{m=1}^{X-1} \beta_{x,m} Gr_{x,m,i}$

642 where  $Gr_{x+z,n,i}$  is the sum of the dosages of two-field alleles in a group  $n$  by a given  
643 combination of the amino acid residues at positions  $x$  and  $z$ .

644 Thus, we define the next most significant amino acid position which additionally and  
645 independently explains the disease risk from the position  $x$ . If the model improvement in this  
646 second round is statistically significant, we iterate the same analyses to identify amino acid  
647 position(s) other than the previously identified positions that best improve the model over the  
648 model including those previous positions, until we obtain no further significant improvement  
649 from any of the remaining positions.

650

651

Sakaue et al.

	<b>a. First round</b>	<b>b. Second round</b>
HLA-DRB1*01:01	RFLWQ <b>L</b> KFECH	DLLEQ <b>R</b> RRAVD
HLA-DRB1*01:02	RFLWQ <b>L</b> KFECH	DLLEQ <b>R</b> RRAVD
HLA-DRB1*03:01	RFLEY <b>S</b> TSECH	DLLEQ <b>K</b> RGRVD
HLA-DRB1*04:01	RFLEQ <b>V</b> KHECH	DLLEQ <b>K</b> RRAAVD
HLA-DRB1*04:03	RFLEQ <b>V</b> KHECH	DLLEQ <b>R</b> RRAEV
HLA-DRB1*04:05	RFLEQ <b>V</b> KHECH	DLLEQ <b>R</b> RRAAVD
HLA-DRB1*04:06	RFLEQ <b>V</b> KHECH	DLLEQ <b>R</b> RRAEV
HLA-DRB1*04:07	RFLEQ <b>V</b> KHECH	DLLEQ <b>R</b> RRAEV
HLA-DRB1*04:10	RFLEQ <b>V</b> KHECH	DLLEQ <b>R</b> RRAAVD
HLA-DRB1*07:01	RFLWQ <b>G</b> KYKCH	DILED <b>R</b> RQQVD
HLA-DRB1*08:01	RFLEY <b>S</b> TGECY	DFLED <b>R</b> RALVD
HLA-DRB1*08:02	RFLEY <b>S</b> TGECY	DFLED <b>R</b> RALVD
HLA-DRB1*08:03	RFLEY <b>S</b> TGECY	DFLED <b>R</b> RALVD
HLA-DRB1*09:01	RFLKQ <b>D</b> KFECH	DFLER <b>R</b> RRAEV
HLA-DRB1*10:01	RFLEE <b>V</b> KFECH	DLLER <b>R</b> RRAAVD
HLA-DRB1*11:01	RFLEY <b>S</b> TSECH	DFLED <b>R</b> RRAAVD
HLA-DRB1*11:04	RFLEY <b>S</b> TSECH	DFLED <b>R</b> RRAAVD
HLA-DRB1*11:06	RFLEY <b>S</b> TSECH	DFLED <b>R</b> RRAAVD
HLA-DRB1*11:11	RFLEY <b>S</b> TSECH	DFLED <b>E</b> RRAAVD
HLA-DRB1*11:13	RFLEY <b>S</b> TSECH	DLLER <b>R</b> RRAAVD
HLA-DRB1*12:01	RFLEY <b>S</b> TGECY	DILED <b>R</b> RRAAVD
HLA-DRB1*12:02	RFLEY <b>S</b> TGECY	DFLED <b>R</b> RRAAVD
HLA-DRB1*13:01	RFLEY <b>S</b> TSECH	DILED <b>E</b> RRAAVD
HLA-DRB1*13:02	RFLEY <b>S</b> TSECH	DILED <b>E</b> RRAAVD
HLA-DRB1*13:03	RFLEY <b>S</b> TSECH	DILED <b>K</b> RRAAVD
HLA-DRB1*14:01	RFLEY <b>S</b> TSECH	DLLER <b>R</b> RRAEV
HLA-DRB1*14:02	RFLEY <b>S</b> TSECH	DLLEQ <b>R</b> RRAAVD
HLA-DRB1*14:05	RFLEY <b>S</b> TSECQ	DLLER <b>R</b> RRAEV
HLA-DRB1*15:01	RFLWQ <b>P</b> KRECH	DILEQ <b>A</b> RAAVD
HLA-DRB1*15:02	RFLWQ <b>P</b> KRECH	DILEQ <b>A</b> RAAVD
HLA-DRB1*15:03	RFLWQ <b>P</b> KRECH	DILEQ <b>A</b> RAAVD
HLA-DRB1*16:02	RFLWQ <b>P</b> KRECH	DLLED <b>R</b> RRAAVD

652

653 **Figure 5. Grouping of two-field alleles in conditional haplotype test**

Sakaue et al.

654 An example illustration of the conditional haplotype test for the *HLA-DRB1* gene. In the first  
655 round of the amino acid association test at position +11 (**a**), we group all two-field alleles (32  
656 alleles in total) into 6 groups based on the amino acid residues at the position +11, and ask  
657 whether those groups significantly explain the disease risk by using omnibus test. In the second  
658 round of conditional haplotype test (**b**; position +71 as an example), we group the two-field  
659 alleles into 10 groups based on the amino acid residues at the position +11 and +71. Then, we  
660 ask whether those 10 groups explain the disease risk more significantly than the 6 groups that  
661 we defined in the first round.

662

Sakaue et al.

663 **Tests for non-additivity**

664 The dosage effect of HLA (having one copy or two copies of a given HLA allele) on disease risk  
665 is not purely additive in infectious diseases and autoimmune diseases<sup>55–63</sup>. All the analyses we  
666 have described above assume the additive risk model, a model in which the risk (i.e., log Odds  
667 Ratio(OR)) for acquiring a disease due to carrying one copy of the allele (heterozygous state) is  
668 half the risk (log(OR)) conferred by carrying two copies (homozygous state). A non-additive  
669 effect represents a deviation from this linear relationship between the dosage and the risk  
670 (**Figure 6a**). For instance, a dominant effect might be indicated when the effect of carrying one  
671 copy is more than half the effect of carrying two copies. A biological explanation for such a  
672 dominant effect might be (1) having one copy is enough to express the MHC variant with the  
673 disease-relevant antigen-binding properties on the cell surface, or that (2) there are synergistic  
674 interactions with another HLA allele at the same locus. Lenz et al.<sup>62,64</sup> showed that such  
675 non-additive effects are pervasive in a spectrum of autoimmune diseases.

676 To test for the non-additive effect, we construct a logistic regression model which captures  
677 both additive and non-additive contribution of the allele to the disease risk (**Figure 6b**)<sup>62,65</sup>. We  
678 first define the additive term  $x_{i,j}$  as either the best guess or the dosage genotype of allele  $j$  in  
679 an individual  $i$  which we are interested in.

$$x_{i,j} = \begin{cases} \text{the best guess genotype of the allele } j \text{ in an individual } i: \{0,1,2\} \\ \text{the dosage genotype of the allele } j \text{ in an individual } i: 0 \leq x_{i,j} \leq 2 \end{cases}$$

680 We next define the non-additive term  $\delta_{i,j}$  as the heterozygous status of the allele  $j$  in an  
681 individual  $i$ , which should capture any deviation of the effect from the additivity.

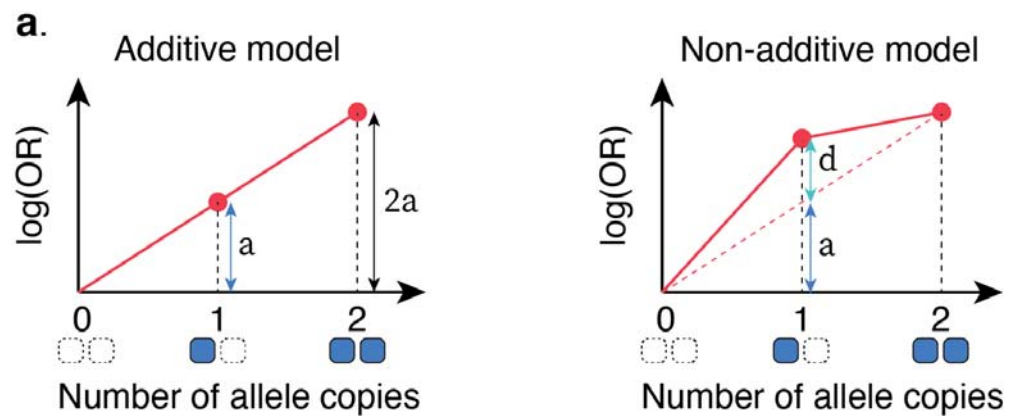
$$\delta_{i,j} = \begin{cases} 1 \text{ if and only if } x_{i,j} = 1, & 0 \text{ otherwise : } \{0,1\} \\ 1 - \text{abs}(1 - x_{i,j}): 0 \leq \delta_{i,j} \leq 2 \end{cases}$$

Sakaue et al.

682

Sakaue et al.

683



**b.**  $\log(\text{odds}_i) = \beta_0 + a_j x_{i,j} + d_j \delta_{i,j} + \sum_k \beta_k x_{k,i} + \sum_l \beta_l PC_{l,i}$

individual	allele j		
$i = 1$	○○	0	0
$i = 2$	○○	1	1
$i = 3$	○○	2	0
$i = 4$	○○	1	1

**c.**  $Y_i = \theta + \sum_k \beta_k x_{k,i} + \sum_l \beta_l PC_{l,i} + \sum_{m=1}^{L-1} \beta_m AM_{m,i}$

phenotypes	amino acid residues
$i = 1$	$\begin{pmatrix} 0 & 2 & 0 & 0 \end{pmatrix}$
$i = 2$	$\begin{pmatrix} 0 & 1 & 0 & 1 \end{pmatrix}$
$i = 3$	$\begin{pmatrix} 0 & 1 & 0 & 0 \end{pmatrix}$
$i = 4$	$\begin{pmatrix} 0 & 0 & 1 & 1 \end{pmatrix}$

684

685 **Figure 6. Non-additive test and multi-trait analysis**

686 **a.** Schematic illustrations of additive model and non-additive models using the log odds ratio  
 687 (log(OR)) according to the dosage of the genotype of interest.  $a$  denotes the purely additive  
 688 effect by having one copy of the allele, and  $d$  denotes any departure from additivity at

Sakaue et al.

689 heterozygous genotype. **b.** A logistic regression model to assess both the additive and  
690 non-additive effect of the allele  $j$  (see main text for details). **c.** Multi-trait analysis by using  
691 multiple linear regression model (MMLM) to test the association between multi-dimensional  
692 phenotype  $Y$  and the amino acid polymorphism.

693

694

Sakaue et al.

695 Using those two terms  $x_{i,j}$  and  $\delta_{i,j}$ , we construct a full model by including both additive and  
696 non-additive term with covariates, and a reduced model with by including only additive term with  
697 covariates.

698 Full model:  $\log(\text{odds}_i) = \beta_0 + a_j x_{i,j} + d_j \delta_{i,j} + \sum_k \beta_k x_{k,i} + \sum_l \beta_l PC_{l,i}$

699 Reduced model:  $\log(\text{odds}_i) = \beta_0 + a_j x_{i,j} + \sum_k \beta_k x_{k,i} + \sum_l \beta_l PC_{l,i}$

700 where  $a_j$  denotes an additive effect and  $d_j$  denotes a non-additive (dominance if positive)  
701 effect.

702 We finally assess the significance of the improvement in model fit of the Full model over the  
703 Reduced model in model fit by the delta deviance (sum of squares) using an F-test.

704

## 705 **Tests for interactions among HLA alleles**

706 Once we identify an allele harboring a possible non-additive effect, we may also be interested in  
707 understanding whether this is due to an interaction effect between the identified allele and the  
708 other allele at the same HLA locus. In other situations, we may want to assess an interaction  
709 effect between a pair of alleles of functional interest. If the disease risk from a combination of  
710 those two alleles deviates from the expected disease risk by multiplying the disease risk (i.e.,  
711 adding the log(OR)) of each of the two alleles, that combination can be regarded as having an  
712 interaction effect. To test this hypothesis, we construct a reduced model which only includes an  
713 additive term for each of the two alleles, and a full model which includes an interaction term  
714 between the two alleles in addition to the additive term for each of the two alleles. Let  $x_{i,j}$  be  
715 the dosage genotype of the allele  $j$  in a given individual  $i$  nominated by a significant

Sakaue et al.

716 non-additive test, and let  $x_{i,h}$  be the dosage genotype of the other allele  $h$  ( $h \neq j$ ) in an  
717 individual  $i$  to be tested for an interaction effect with the allele  $j$ .

718 Full model:  $\log(\text{odds}_i) = \beta_0 + a_j x_{i,j} + a_h x_{i,h} + \phi_{j,h} x_{i,j} x_{i,h} + \sum_k \beta_k x_{k,i} + \sum_l \beta_l PC_{l,i}$

719 Reduced model:  $\log(\text{odds}_i) = \beta_0 + a_j x_{i,j} + a_h x_{i,h} + \sum_k \beta_k x_{k,i} + \sum_l \beta_l PC_{l,i}$

720 where  $\phi_{j,h}$  is the effect size of the interaction between the alleles  $j$  and  $h$ . We again assess  
721 the significance of the improvement in Full model over Reduced model in model fit by the delta  
722 deviance (sum of squares) using an F-test. We note that the observed interaction effects can be  
723 spurious when the frequencies of the tested alleles are relatively low, which results in noisy  
724 effect estimate. We consider conservative QC of the tested alleles based on MAF (e.g., MAF >  
725 0.05 or 0.10), or performing permutation analyses to test whether the observed statistics could  
726 occur by chance, in such cases.

727

## 728 **HLA evolutionary allele divergence**

729 A potential source for non-additive interaction effects among HLA alleles is the extent to which  
730 their encoded HLA molecule variants differ functionally (i.e., in their bound antigen repertoires).

731 Since HLA genes are generally co-dominantly expressed, both HLA variants of a heterozygous  
732 individual are presenting antigens at the cell surface. If two HLA alleles are very similar in their  
733 sequence, their encoded HLA molecules on average will bind similar sets of antigens and thus  
734 exhibit a substantial overlap in their presented antigen repertoires, while the opposite will be  
735 true for two alleles with very divergent sequences<sup>66</sup>. The concept that carrying two divergent  
736 HLA alleles will allow HLA-presentation of a wider range of antigens, and by extension increase

Sakaue et al.

737 the likelihood of pathogen detection by the adaptive immune system, has been termed  
738 *divergent allele advantage* (DAA), as an extension of the classical heterozygote advantage<sup>67,68</sup>.  
739 DAA has already been shown to drive HLA allele frequencies and contribute to HIV control<sup>63,66</sup>.  
740 but might have broader implications in HLA-mediated complex diseases. For instance, it was  
741 shown that cancer patients whose HLA class I alleles exhibit a higher HLA evolutionary  
742 divergence (HED) respond better to cancer immunotherapy, possibly because more mutated  
743 neoantigens are presented by their HLA<sup>69</sup>. The HED score between two HLA alleles at a given  
744 HLA locus is based on the Grantham distance between their amino acid sequences. The HED  
745 is applicable to both HLA class I and class II alleles. It can be calculated using publicly available  
746 scripts<sup>66</sup>, and its effect on a given phenotype can then be estimated by adding it as a  
747 quantitative parameter in a regression model and testing for improvement in model fit with an  
748 F-test.

749

## 750 **Multi-trait analysis**

751 Our group recently showed that the amino acid frequencies at complementarity-determining  
752 region 3 (CDR3) of the T cell receptor (TCR) are highly influenced by the HLA alleles and amino  
753 acids, possibly through thymic selection<sup>6</sup>. This type of analysis is an extension of the analyses  
754 we described in the previous sections. One notable difference is that the response variable  
755 represents not a single trait (e.g., a disease) but multiple traits: in this case the frequencies of  
756 each amino acid residue at the position of interest within CDR3, which we call cdr3-QTL

Sakaue et al.

757 analysis. We test which amino acid position has a significant association with those frequencies  
758 overall, using an extended framework of the omnibus test that we described above (**Figure 6c**).

759 In this case, the response variable is not a vector of one phenotype, but a matrix  
760 (multidimensional vector) of frequency phenotypes where each row represents an individual  
761 and each column represents a frequency of a given amino acid residue at a given position of  
762 CDR3. Let  $Y$  be this frequency matrix with  $N$  rows and  $M - 1$  columns, and  $Y_i$  be the  $M - 1$   
763 frequency phenotypes in an individual  $i$ .  $N$  denotes the number of individuals, and  $M$  denotes  
764 the number of observed amino acid residues at this position. We perform a multivariate multiple  
765 linear regression model (MMLM) to test the association between  $Y$  and HLA alleles or amino  
766 acid positions of interest.

767 Full model:  $Y_i = \theta + \sum_k \beta_k x_{k,i} + \sum_l \beta_l PC_{l,i} + \sum_{m=1}^{L-1} \beta_m AM_{m,i}$

768 Reduced model:  $Y_i = \theta + \sum_k \beta_k x_{k,i} + \sum_l \beta_l PC_{l,i}$

769 where  $\theta$  is an  $M$ -dimensional parameter that represents the intercept,  $L$  is the total number of  
770 observed amino acid polymorphisms at this position,  $AM_{m,i}$  and  $\beta_m$  are the amino acid  
771 dosage of the residue  $m$  in an individual  $i$  and the  $M$ -dimensional effect sizes for the residue  
772  $m$  on  $Y$ , respectively.

773 We assess the significance of the improvement in model fit between Full model and  
774 Reduced model with the multivariate analysis of variance (MANOVA) test for quantitative traits.  
775 As spurious associations again arise when the frequencies of the tested alleles are relatively  
776 low<sup>6</sup>, we recommend performing permutation analyses to confirm the calibration of the test  
777 statistics.

Sakaue et al.

778 By using this multi-trait framework, we can assess any combination of multiple phenotypes.

779 One potential application is to investigate disease phenotypes by using deep phenotype record

780 in biobanks. This framework could disentangle pleiotropic HLA alleles that simultaneously affect

781 a spectrum of diseases of interest. Another interesting application might be multiple molecular

782 phenotypes such as expression or protein abundance of multiple genes, and a combination of

783 multiple modalities (e.g., expression and chromatin accessibility). We can also assess those

784 phenotypes across multiple cell types (e.g., expression of a gene in T cells, B cells, Monocytes

785 etc.).

786

### 787 **Concluding remarks**

788 Given the increasing number of associations between the HLA region and human complex

789 traits that have been identified through large-scale GWAS, accurate imputation and

790 fine-mapping of the causal HLA alleles and amino acids will continue to be important as the

791 data size continues to grow. We present a strategy that can lead investigators to fine-mapped

792 alleles. Leveraging HLA fine-mapped alleles with the variants outside of MHC region, it may be

793 possible to construct an efficient genetic risk score to stratify people based on the genetic risk

794 for those diseases. We have publicized this imputation pipeline through the user-friendly MIS,

795 which hosts the HLA reference panel representing multiple populations and enables web-based

796 automatic HLA imputation for global cohorts. Another advantage of this implementation is the

797 computational efficiency: HLA imputation of a cohort of millions of individuals is computationally

798 scalable (for example, for a cohort of size 20,000, HLA imputation runs within 1 hour). We hope

Sakaue et al.

799 this protocol will empower the field of statistical genetics to more comprehensively define the  
800 effect of HLA variation on a spectrum of human diseases.

801 Despite the well-established performance of our approach, we can still improve our HLA  
802 imputation reference panel further. First, we continue to expand the reference panel to better  
803 represent global populations that are currently missing (e.g., Africans and South Asians).  
804 Similarly, the scope of genes included in the panel can be expanded to include, for example,  
805 non-classical *HLA* genes and *C4* copy number. Second, the imputation accuracy is currently  
806 satisfactory in association testing but not yet as high as the gold-standard HLA typing. We aim  
807 to further improve the accuracy by updating the HLA calls and scaffold variants used in the  
808 reference panel as well as improving the imputation algorithms.

809 While fine-mapping of HLA alleles has provided deeper insights into disease pathogenesis,  
810 we need more mechanistic or structural understanding of how these alleles contribute to  
811 disease biology. Why do certain HLA alleles cause a diverse spectrum of diseases? How do  
812 those alleles characterize our inherited composition of T cell repertoires? What are  
813 auto-antigens that are being presented by those alleles? Recent advances in experimental and  
814 computational modeling of protein structures and its complex<sup>70,71</sup> can offer promise. We need  
815 both experimental and computational approaches to answer all these important questions.

816

817 **Data Availability**

Sakaue et al.

818 We provided the availability of HLA imputation reference panel at Table 1. We made our HLA  
819 imputation pipeline using multi-ancestry HLA reference panel publicly available at Michigan  
820 Imputation Server (<https://imputationserver.sph.umich.edu/index.html>).

821

## 822 **Code Availability**

823 The computational scripts and their usage related to this tutorial are available at  
824 [https://github.com/immunogenomics/HLA\\_analyses\\_tutorial](https://github.com/immunogenomics/HLA_analyses_tutorial).

825

## 826 **References**

- 827 1. Trowsdale, J. & Knight, J. C. Major histocompatibility complex genomics and human  
828 disease. *Annu Rev Genomics Hum Genet* **14**, 301–323 (2013).
- 829 2. Amiel, J. Study of the Leukocyte Phenotypes in Hodgkin's Disease. in *Histocompatibility*  
830 *testing* (ed. Teraski, P. I.) 79–81 (Munksgaard, 1967).
- 831 3. Murphy, K. & Weaver, C. Janeway 's Immunology. *America (NY)* 1–277 (2017).
- 832 4. Dendrou, C. A., Petersen, J., Rossjohn, J. & Fugger, L. HLA variation and disease. *Nature*  
833 *Reviews Immunology* **2017 18:5** **18**, 325–339 (2018).
- 834 5. Scally, S. W. *et al.* A molecular basis for the association of the HLA-DRB1 locus,  
835 citrullination, and rheumatoid arthritis. *Journal of Experimental Medicine* **210**, 2569–2582  
836 (2013).
- 837 6. Ishigaki, K. *et al.* HLA autoimmune risk alleles restrict the hypervariable region of T cell  
838 receptors. *Nature Genetics* **2022 54:4** **54**, 393–402 (2022).
- 839 7. McGonagle, D., Aydin, S. Z., Güll, A., Mahr, A. & Direskeneli, H. 'MHC-I-opathy'-unified  
840 concept for spondyloarthritis and Behçet disease. *Nat Rev Rheumatol* **11**, 731–740  
841 (2015).
- 842 8. Sekar, A. *et al.* Schizophrenia risk from complex variation of complement component 4.  
843 *Nature* **530**, 177 (2016).
- 844 9. Sakaue, S. *et al.* A cross-population atlas of genetic associations for 220 human  
845 phenotypes. *Nature Genetics* **53**, 1415–1424 (2021).

Sakaue et al.

- 846 10. Luo, Y. *et al.* A high-resolution HLA reference panel capturing global population diversity  
847 enables multi-ancestry fine-mapping in HIV host response. *Nat Genet* **53**, 1504–1516  
848 (2021).
- 849 11. Das, S. *et al.* Next-generation genotype imputation service and methods. *Nature Genetics*  
850 **48**, 1284–1287 (2016).
- 851 12. Raychaudhuri, S. *et al.* Five amino acids in three HLA proteins explain most of the  
852 association between MHC and seropositive rheumatoid arthritis. *Nature Genetics* **44**,  
853 291–296 (2012).
- 854 13. Robinson, J. *et al.* IPD-IMGT/HLA Database. *Nucleic Acids Res* **48**, D948–D955 (2020).
- 855 14. Marsh, S. G. E. *et al.* Nomenclature for factors of the HLA system, 2010. *Tissue Antigens*  
856 **75**, 291 (2010).
- 857 15. Marchini, J. & Howie, B. Genotype imputation for genome-wide association studies. *Nat  
858 Rev Genet* **11**, 499–511 (2010).
- 859 16. Fleischhauer, K., Zino, E., Bordignon, C. & Benazzi, E. Complete generic and extensive  
860 fine-specificity typing of the HLA-B locus by the PCR-SSOP method. *Tissue Antigens* **46**,  
861 281–292 (1995).
- 862 17. Dilthey, A. T. *et al.* High-Accuracy HLA Type Inference from Whole-Genome Sequencing  
863 Data Using Population Reference Graphs. *PLOS Computational Biology* **12**, e1005151  
864 (2016).
- 865 18. Dilthey, A. T. *et al.* HLA\*LA—HLA typing from linearly projected graph alignments.  
866 *Bioinformatics* **35**, 4394–4396 (2019).
- 867 19. Jia, X. *et al.* Imputing Amino Acid Polymorphisms in Human Leukocyte Antigens. *PLoS  
868 ONE* **8**, e64683 (2013).
- 869 20. Zheng, X. *et al.* HIBAG—HLA genotype imputation with attribute bagging. *The  
870 Pharmacogenomics Journal 2014 14:2* **14**, 192–200 (2013).
- 871 21. Dilthey, A. T., Moutsianas, L., Leslie, S. & McVean, G. HLA\*IMP—an integrated  
872 framework for imputing classical HLA alleles from SNP genotypes. *Bioinformatics* **27**, 968  
873 (2011).
- 874 22. Shen, J. J. *et al.* HLA-IMPUTER: an easy to use web application for HLA imputation and  
875 association analysis using population-specific reference panels. *Bioinformatics* **35**,  
876 1244–1246 (2019).

Sakaue et al.

- 877 23. Maiers, M. *et al.* GRIMM: GRaph IMputation and matching for HLA genotypes.  
878 *Bioinformatics* **35**, 3520–3523 (2019).
- 879 24. Breiman, L. Bagging predictors. *Machine Learning* **1996 24:2** **24**, 123–140 (1996).
- 880 25. Pillai, N. E. *et al.* Predicting HLA alleles from high-resolution SNP data in three Southeast  
881 Asian populations. *Hum Mol Genet* **23**, 4443–4451 (2014).
- 882 26. Hirata, J. *et al.* Genetic and phenotypic landscape of the major histocompatibility complex  
883 region in the Japanese population. *Nature Genetics* **51**, 470–480 (2019).
- 884 27. Zhou, F. *et al.* Deep sequencing of the MHC region in the Chinese population contributes  
885 to studies of complex disease. *Nat Genet* **48**, 740–746 (2016).
- 886 28. Kim, K., Bang, S. Y., Lee, H. S. & Bae, S. C. Construction and Application of a Korean  
887 Reference Panel for Imputing Classical Alleles and Amino Acids of Human Leukocyte  
888 Antigen Genes. *PLOS ONE* **9**, e112546 (2014).
- 889 29. Dilthey, A., Cox, C., Iqbal, Z., Nelson, M. R. & McVean, G. Improved genome inference in  
890 the MHC using a population reference graph. *Nature Genetics* **47**, 682–688 (2015).
- 891 30. Verlouw, J. A. M. *et al.* A comparison of genotyping arrays. *European Journal of Human  
892 Genetics* **29**, 1611 (2021).
- 893 31. Vince, N. *et al.* SNP-HLA Reference Consortium (SHLARC): HLA and SNP data sharing  
894 for promoting MHC-centric analyses in genomics. *Genetic Epidemiology* **44**, 733–740  
895 (2020).
- 896 32. Klareskog, L., Catrina, A. I. & Paget, S. Rheumatoid arthritis. *Lancet* **373**, 659–672 (2009).
- 897 33. Padyukov, L. *et al.* A genome-wide association study suggests contrasting associations in  
898 ACPA-positive versus ACPA-negative rheumatoid arthritis. *Annals of the Rheumatic  
899 Diseases* **70**, 259–265 (2011).
- 900 34. Bycroft, C. *et al.* The UK Biobank resource with deep phenotyping and genomic data.  
901 *Nature* **562**, 203–209 (2018).
- 902 35. Wu, P. *et al.* Mapping ICD-10 and ICD-10-CM Codes to Phecodes: Workflow  
903 Development and Initial Evaluation. *JMIR Med Inform* **2019;7(4):e14325**  
904 <https://medinform.jmir.org/2019/4/e14325> **7**, e14325 (2019).
- 905 36. Gutierrez-Arcelus, M. *et al.* Allele-specific expression changes dynamically during T cell  
906 activation in HLA and other autoimmune loci. *Nat Genet* **52**, 247 (2020).
- 907 37. D'Antonio, M. *et al.* Systematic genetic analysis of the MHC region reveals mechanistic  
908 underpinnings of HLA type associations with disease. *Elife* **8**, (2019).

Sakaue et al.

- 909 38. Aguiar, V. R. C., César, J., Delaneau, O., Dermitzakis, E. T. & Meyer, D. Expression  
910 estimation and eQTL mapping for HLA genes with a personalized pipeline. *PLOS*  
911 *Genetics* **15**, e1008091 (2019).
- 912 39. Anderson, C. A. *et al.* Data quality control in genetic case-control association studies.  
913 *Nature Protocols* **5**, 1564–1573 (2010).
- 914 40. Marees, A. T. *et al.* A tutorial on conducting genome-wide association studies: Quality  
915 control and statistical analysis. *Int J Methods Psychiatr Res* **27**, (2018).
- 916 41. Hinrichs, A. S. *et al.* The UCSC Genome Browser Database: update 2006. *Nucleic Acids*  
917 *Res* **34**, (2006).
- 918 42. Gibbs, R. A. *et al.* A global reference for human genetic variation. *Nature* **526**, 68–74  
919 (2015).
- 920 43. Karczewski, K. J. *et al.* The mutational constraint spectrum quantified from variation in  
921 141,456 humans. *Nature* **581**, 434–443 (2020).
- 922 44. Gomes, I. *et al.* Hardy-Weinberg quality control. *Ann Hum Genet* **63**, 535–538 (1999).
- 923 45. Hosking, L. *et al.* Detection of genotyping errors by Hardy-Weinberg equilibrium testing.  
924 *Eur J Hum Genet* **12**, 395–399 (2004).
- 925 46. Wittke-Thompson, J. K., Pluzhnikov, A. & Cox, N. J. Rational Inferences about Departures  
926 from Hardy-Weinberg Equilibrium. *American Journal of Human Genetics* **76**, 967 (2005).
- 927 47. Galinsky, K. J. *et al.* Fast Principal-Component Analysis Reveals Convergent Evolution of  
928 ADH1B in Europe and East Asia. *Am J Hum Genet* **98**, 456–472 (2016).
- 929 48. Cook, S. *et al.* Accurate imputation of human leukocyte antigens with CookHLA. *Nature*  
930 *Communications* **2021 12:1 12**, 1–11 (2021).
- 931 49. Browning, S. R. & Browning, B. L. Rapid and accurate haplotype phasing and  
932 missing-data inference for whole-genome association studies by use of localized  
933 haplotype clustering. *American Journal of Human Genetics* **81**, 1084–1097 (2007).
- 934 50. Delaneau, O., Zagury, J. F. & Marchini, J. Improved whole-chromosome phasing for  
935 disease and population genetic studies. *Nature Methods* **10**, 5–6 (2013).
- 936 51. Loh, P.-R. *et al.* Reference-based phasing using the Haplotype Reference Consortium  
937 panel. *Nature Genetics* **48**, 1443–1448 (2016).
- 938 52. Purcell, S. *et al.* PLINK: A Tool Set for Whole-Genome Association and Population-Based  
939 Linkage Analyses. *The American Journal of Human Genetics* **81**, 559–575 (2007).

Sakaue et al.

- 940 53. Zhou, W. *et al.* Efficiently controlling for case-control imbalance and sample relatedness in  
941 large-scale genetic association studies. *Nat Genet* **50**, 1335–1341 (2018).
- 942 54. Loh, P. R. *et al.* Efficient Bayesian mixed-model analysis increases association power in  
943 large cohorts. *Nature Genetics* **47**, 284–290 (2015).
- 944 55. Wordsworth, P. *et al.* HLA heterozygosity contributes to susceptibility to rheumatoid  
945 arthritis. *American Journal of Human Genetics* **51**, 585 (1992).
- 946 56. Koeleman, B. P. C. *et al.* Genotype effects and epistasis in type 1 diabetes and HLA-DQ  
947 trans dimer associations with disease. *Genes Immun* **5**, 381–388 (2004).
- 948 57. Thomson, G. *et al.* Relative predispositional effects of HLA class II DRB1-DQB1  
949 haplotypes and genotypes on type 1 diabetes: a meta-analysis. *Tissue Antigens* **70**,  
950 110–127 (2007).
- 951 58. Woelfing, B., Traulsen, A., Milinski, M. & Boehm, T. Does intra-individual major  
952 histocompatibility complex diversity keep a golden mean? *Philos Trans R Soc Lond B Biol  
953 Sci* **364**, 117–128 (2009).
- 954 59. Lipsitch, M., Bergstrom, C. T. & Antia, R. Effect of human leukocyte antigen heterozygosity  
955 on infectious disease outcome: the need for allele-specific measures. *BMC Med Genet* **4**,  
956 (2003).
- 957 60. Tsai, S. & Santamaria, P. MHC Class II Polymorphisms, Autoreactive T-Cells, and  
958 Autoimmunity. *Front Immunol* **4**, (2013).
- 959 61. Goyette, P. *et al.* High-density mapping of the MHC identifies a shared role for  
960 HLA-DRB1\*01:03 in inflammatory bowel diseases and heterozygous advantage in  
961 ulcerative colitis. *Nat Genet* **47**, 172–179 (2015).
- 962 62. Lenz, T. L. *et al.* Widespread non-additive and interaction effects within HLA loci modulate  
963 the risk of autoimmune diseases. *Nature Genetics* **47**, 1085–1090 (2015).
- 964 63. Arora, J. *et al.* HLA Heterozygote Advantage against HIV-1 Is Driven by Quantitative and  
965 Qualitative Differences in HLA Allele-Specific Peptide Presentation. *Mol Biol Evol* **37**,  
966 639–650 (2020).
- 967 64. Hu, X. *et al.* Additive and interaction effects at three amino acid positions in HLA-DQ and  
968 HLA-DR molecules drive type 1 diabetes risk. *Nat Genet* **47**, 898–905 (2015).
- 969 65. Reynolds, E. G. M. *et al.* Non-additive association analysis using proxy phenotypes  
970 identifies novel cattle syndromes. *Nature Genetics* **2021** *53*:7 **53**, 949–954 (2021).

Sakaue et al.

- 971 66. Pierini, F. & Lenz, T. L. Divergent Allele Advantage at Human MHC Genes: Signatures of  
972 Past and Ongoing Selection. *Mol Biol Evol* **35**, 2145–2158 (2018).
- 973 67. Wakeland, E. K. *et al.* Ancestral polymorphisms of MHC class II genes: divergent allele  
974 advantage. *Immunol Res* **9**, 115–122 (1990).
- 975 68. Radwan, J., Babik, W., Kaufman, J., Lenz, T. L. & Winternitz, J. Advances in the  
976 Evolutionary Understanding of MHC Polymorphism. *Trends Genet* **36**, 298–311 (2020).
- 977 69. Chowell, D. *et al.* Evolutionary divergence of HLA class I genotype impacts efficacy of  
978 cancer immunotherapy. *Nat Med* **25**, 1715–1720 (2019).
- 979 70. Nakane, T. *et al.* Single-particle cryo-EM at atomic resolution. *Nature* **2020** 587:7832 **587**,  
980 152–156 (2020).
- 981 71. Jumper, J. *et al.* Highly accurate protein structure prediction with AlphaFold. *Nature* **2021**  
982 596:7873 **596**, 583–589 (2021).
- 983

#### 984 **Acknowledgments**

985 This work is supported in part by funding from the National Institutes of Health (R01AR063759,  
986 U01HG012009, UC2AR081023). S.Sakaue was in part supported by the Manabe Scholarship  
987 Grant for Allergic and Rheumatic Diseases and the Uehara Memorial Foundation. J.B.K. was  
988 supported by NIH/NIGMS T32GM007753. A.J.D. was funded by NIH/NIDDK T32DK007028.  
989 T.L.L. was funded by the Deutsche Forschungsgemeinschaft (DFG, German Research  
990 Foundation) – Projektnummer 437857095.

991

#### 992 **Author Contributions**

993 S.Sakaue and S.R. conceived the work and wrote the manuscript with critical input from all  
994 authors. S.Sakaue and S.G. created a web tutorial accompanying this manuscript. All authors  
995 contributed to developing this protocol. S.Sakaue, M.C., Y.L., W.C., S.Schönherr, L.F., J.L.,

Sakaue et al.

996 C.F., A.V.S., and S.R. contributed to updating the multi-ancestry HLA reference panel and  
997 implementing HLA imputation at Michigan Imputation Server.

998

999 **Competing Financial Interests**

1000 B.H. is a CTO of Genealogy Inc. T.L.L. is a co-inventor on a patent application for using HED in  
1001 predicting cancer immunotherapy success.

1002